CONFIDENTIAL

NACA RM A50I14

NACA

RESEARCH MEMORANDUM

WIND-TUNNEL INVESTIGATION AT LOW SPEED OF A WING SWEPT BACK 63° AND TWISTED AND CAMBERED FOR UNIFORM LOAD AT A LIFT COEFFICIENT OF 0.5 AND WITH A THICKENED TIP SECTION

By James A. Weiberg and Hubert C. Carel

Ames Aeronautical Laboratory
Moffett Field, Calif.

NATIONAL ADVISORY COMMITTEE
FOR AERONAUTICS

WASHINGTON
November 21, 1950

CONFIDENTIAL

NATIONAL ADVISORY COMMITTEE FOR AERONAUTICS

RESEARCH MEMORANDUM

WIND-TUNNEL INVESTIGATION AT LOW SPEED OF A WING SWEPT BACK 63° AND TWISTED AND CAMBERED FOR UNIFORM LOAD AT A LIFT COEFFICIENT OF 0.5 AND WITH A THICKENED TIP SECTION

By James A. Weiberg and Hubert C. Carel

SUMMARY

Tests were made to determine the longitudinal-stability characteristics and the spanwise distribution of load of a semispan model of a wing with the leading edge swept back 63° and with a thickened tip section. The wing was twisted and cambered to produce an approximately uniform lift distribution at a lift coefficient of 0.5 and at a Mach number of 1.4. Tests were also made of the wing with a fuselage and with various devices for altering the stall and spanwise boundary-layer flow.

Comparisons with the results of tests of the wing, made before the addition of thickness to the tip sections, showed that the increased thickness and slightly altered twist from midsemispan to the tip of the wing resulted in reduced tip-leading-edge pressure peaks with no improvement of tip lift characteristics. Thus, the early loss of lift of wing sections near the tip which resulted in the large variations in longitudinal stability was attributable largely to spanwise flow of the boundary layer rather than to local stall of the tip sections. Hence, the expected improvement of the longitudinal stability of the wing was not realized.

The addition of flaps and upper-surface fences to the wing for stall and boundary-layer control considerably improved the stability characteristics of the wing.

The change of spanwise variation of twist and thickness had little effect on the spanwise distribution of load.

INTRODUCTION

The merits of large amounts of sweep for efficient flight (i.e., for reasonably high lift-drag ratios) at moderate supersonic speeds have been

demonstrated by wind-tunnel tests of a wing with the leading edge swept back 63° (references 1 and 2). At low subsonic Mach numbers this wing is characterized by large variations of longitudinal stability with angle of attack even at low lift coefficients (references 3 and 4). These stability variations were attributed in reference 3 to spanwise flow in the boundary layer and to flow separation at wing sections near the tip. Twisting and cambering the wing a moderate amount to relieve the load at the tip and to obtain a more uniform distribution of load at a moderately low lift coefficient (0.25 at a Mach number of 1.5) resulted in higher lift-drag ratios at supersonic speeds (reference 5) but provided little improvement of the stability characteristics at subsonic speeds (reference 6). Tests of a wing twisted and cambered for uniform load at a moderately high lift coefficient (0.5 at a Mach number of 1.4) likewise showed no improvement of the stability characteristics at low subsonic Mach numbers (reference 7).

In reference 7, the poor stability characteristics of the wing at comparatively low lift coefficients were attributed to the inability of the wing sections near the tip to maintain lift without flow separation to sufficiently high angles of attack.

Subsequent to the tests of reference 7 it was reasoned that the lift range for satisfactory stability characteristics might be extended to higher lift coefficients by increasing the range of usable lift of the sections near the tip through an increase of the thickness of these sections. Computations showed that the increase of drag at supersonic speeds due to the increased thickness of sections near the tip would be relatively small.

Consequently, the model used for the research reported in reference 7 was altered to incorporate thicker sections from the midsemispan to the tip. For expediency in model construction, the twist of the revised portion of the wing was also modified from that of the original wing.

Tests of the wing were made in one of the Ames 7- by 10-foot wind tunnels. The longitudinal characteristics of this wing as shown by force and pressure-distribution measurements are presented herein. Also included are the effects of a fuselage, of upper-surface fences, of spoilers, of elevons, and of a leading-edge flap on the low-speed characteristics of the wing.

NOTATION

All data are presented as NACA coefficients. The angle of attack and lift, drag, and pitching-moment coefficients are corrected for tunnel-wall effects. Forces and moments are those for the semispan model and are referred to the wind axis and to the moment center shown in figure 1. Coefficients and symbols used are defined as follows:

A aspect ratio $\left(\frac{b^2}{S}\right)$

b span of complete wing measured perpendicular to the plane of symmetry[1] (twice span of semispan wing), feet

c' wing chord (fig. 2), feet

c projection of wing chord in wing reference plane[2] (c' cos ϵ, fig. 2)[3], feet

$\bar{c}$ mean aerodynamic chord $\left(\frac{\int_0^{b/2} c^2 dy}{\int_0^{b/2} c\, dy}\right)$, feet

c_{av} average chord $\left(\frac{S}{b}\right)$, feet

C_D drag coefficient $\left[\frac{\text{drag}}{q(S/2)}\right]$

C_L lift coefficient $\left[\frac{\text{lift}}{q(S/2)}\right]$

c_l section lift coefficient

C_{L_α} rate of change of wing lift coefficient with angle of attack $\left(\frac{dC_L}{d\alpha}\right)$

c_{l_α} rate of change of section lift coefficient with wing angle of attack $\left(\frac{dc_l}{d\alpha}\right)$

C_m pitching-moment coefficient about the moment center shown in figure 1 $\left[\frac{\text{pitching moment}}{q\bar{c}(S/2)}\right]$

L/D lift-drag ratio

P pressure coefficient $\left(\frac{p_l - p}{q}\right)$

---

[1]The plane of symmetry contains the X and Z axes (fig. 2).
[2]The wing reference plane contains the wing leading edge and the X and Y axes (fig. 2).
[3]Chord c is parallel to the X axis.

---

p free-stream static pressure, pounds per square foot

p_l local static pressure, pounds per square foot

q dynamic pressure $\left(\frac{\rho V^2}{2}\right)$, pounds per square foot

R Reynolds number $\left(\frac{Vc}{\nu}\right)$

S area of complete wing (twice area of semispan model not including areas of extended-chord elevons or leading-edge flaps), square feet

V free-stream velocity, feet per second

x distance measured parallel to X axis (fig. 2), feet

y distance measured perpendicular to plane of symmetry, feet

$y_{c_{max}}$ maximum mean-line ordinate (fig. 2), percent chord (c')

α angle of attack of wing reference plane, degrees

ϵ angle of twist (fig. 2), degrees

λ taper ratio, ratio of tip chord to root chord

ν kinematic viscosity of air, feet squared per second

ρ mass density of air, slugs per cubic foot

CORRECTIONS

Tunnel-wall corrections were applied to the angle of attack and to the lift, drag, and pitching-moment coefficients using methods similar to those of references 8 and 9. The following corrections were applied:

$$C_L = 0.991\ C_{L_u}$$
$$\alpha = \alpha_u + \Delta\alpha_T$$
$$C_m = C_{m_u} + \Delta C_{m_T}$$
$$C_D = C_{D_u} + \Delta C_{D_T}$$

where

$$\Delta\alpha_T = 1.358 \left(C_{L_u}\right)_{w+f} + 0.190 \left(C_{L_u}\right)_{w}$$

$$\Delta C_{m_T} = 0.0010\, C_{L_u}$$

$$\Delta C_{D_T} = 0.0319\, C_{L_u}{}^2$$

and the subscripts signify

u uncorrected

w wing

f flap

No corrections were applied to the data for the effects of model distortion or for possible effects of interference between the model and the tunnel floor or of leakage through the gap between the tunnel floor and the extension of the base of the model where it passed through the floor. These effects were discussed in reference 7 and were believed to have been small. An investigation was made to determine the effect on the wing pressure distribution of the leakage through the tunnel-floor gap. The results are discussed in the section entitled "Pressure-Distribution Measurements."

MODEL DESCRIPTION

The model used in these tests, hereinafter referred to as the revised wing (figs. 1 and 3), was the model described in reference 7, hereinafter referred to as the original wing, with the twist and thickness altered from the midsemispan to the tip. The wing tested was a semispan model with 63° sweepback of the leading edge, an aspect ratio of 3.5, and a taper ratio of 0.25 (ratio of tip chord to root chord). The thickness distribution of the tip section of the revised wing parallel to the plane of symmetry was that of the NACA 0012 section. The camber line of the tip section and the camber line of the section at midsemispan parallel to the plane of symmetry on the revised wing were the same as on the original wing.[4] (See fig. 4.)

[4]The thickness distribution of sections on the original wing in planes perpendicular to the wing leading edge was that of the NACA 0010 section (5.7-percent-thick sections parallel to the plane of symmetry).

For expediency in model construction, constant-percent-chord lines on the surface of the revised wing were straight from midsemispan to the tip. This method of construction resulted in a change of twist of the revised portion of the wing. A comparison of the spanwise variations of twist and of the maximum camber and thickness of the sections (parallel to the plane of symmetry) of the original and revised wings is shown in figure 4. Dimensions of the wing are given in figure 1 and table I. The wing was constructed of laminated mahogany and is shown mounted in the tunnel in figure 3. The model was mounted with the tunnel floor as a reflection plane, the plane of symmetry of the wing being coincident with the tunnel floor. There was a gap of 1/8 to 1/4 inch between the tunnel floor and the extension of the base of the model where it passed through the floor to support the model. The wing was equipped with pressure orifices on sections parallel to the plane of symmetry at 0.200, 0.383, 0.707, and 0.924 semispan. The chordwise locations of the pressure orifices are shown in table I.

The fuselage described in reference 7 was tested with the revised wing and is shown in figure 3 mounted on the wing in the tunnel. Dimensions of the fuselage are given in figure 1 and tables II and III. The geometry of the stall-control devices tested on the model is shown in figure 5.

RESULTS AND DISCUSSION

Force Measurements

The data presented herein were obtained at a Reynolds number of 3.7 million based on the wing mean aerodynamic chord (1.3 million based on the tip chord), corresponding, under the test conditions, to a Mach number of 0.16. The maximum angle of attack of the model was limited for structural reasons to 20°. This angle of attack is below that for maximum lift. As a comparison, an uncambered and untwisted wing of the same plan form (reference 4) had a maximum lift coefficient of 1.4 at 36° angle of attack.

The effects of the change of thickness and twist on the aerodynamic characteristics of the wing and the wing with fuselage are shown in figures 6 and 7. The data in these figures for the original wing are from reference 7. As shown by the slopes of the pitching-moment curves in figure 6, the variations of aerodynamic-center location with lift on the original wing were not markedly altered by the change of thickness and twist of the outer half of the semispan wing. The drag of the wing also was not greatly affected by the modification, as shown in figure 7.

The principal effects of adding the fuselage to the wing are shown in figure 8. These effects were a decrease of the negative angle of attack

for zero lift from -7° to -5°, an increase of the lift-curve slope by approximately 0.005 (measured at zero lift), and a decrease of the pitching-moment coefficient at zero lift from approximately 0.06 to 0.01 with little change of static longitudinal stability (dC_m/dC_L). These effects were similar to those obtained by the addition of the fuselage to the original wing (reference 7).

Numerous investigations (e.g., references 4, 10, and 11) have shown that the unsatisfactory stability and stalling characteristics of swept wings at low speeds can be considerably alleviated by the use of leading- and trailing-edge flaps and upper-surface fences for stall and boundary-layer control. Preliminary tests (reference 7) of several such devices on the twisted and cambered wing with 63° sweepback showed promising results. In the present investigation, additional devices (fig. 5) were tested on the wing and the results are presented in figure 9.

The effects of various arrangements of upper-surface fences on the longitudinal stability of the wing are shown in figure 9(a). The data in this figure indicate that a fence on the inner portion of the wing span was nearly as effective as a fence near the tip for reducing the wing instability at lift coefficients between 0.4 and 0.6. Fences at 0.6 and 0.8 semispan extending either over the after 50 percent of the wing chord or over 100-percent chord resulted in the straightest pitching-moment curves to a lift coefficient of about 0.7. The preceding indicates that the spanwise boundary-layer flow which probably affects the load carried by the tip (reference 7) originated largely on the inner portion of the wing span and was more pronounced on the afterportion of the wing chord. Evidence of this flow was also obtained from observations of tufts on the wing. Alining the fence more nearly with the direction of flow over the wing near zero lift (the flow direction as indicated in reference 12 and from observations of tufts) did not improve the effectiveness of the fence as may be seen by comparison of the results obtained with fences A and B (fig. 9(a).

The effectiveness of two types of split-flap elevons deflected upward for reducing the stability variations above a lift coefficient of 0.4 is shown in figure 9(b). The effectiveness of these elevons for producing pitching moments decreased rapidly with increasing lift coefficient above 0.4, and became negligible above a lift coefficient of 0.6. Above a lift coefficient of 0.4 this decrease with lift of the effectiveness of the elevon was accompanied by a nearly linear variation of pitching-moment coefficient with lift of the wing with the extended-chord elevon. Similar results are shown in reference 10 for an upper-surface split flap on a 42° swept-back wing ($A = 4$, $\lambda = 0.6$).

The data in figure 9(b) show that chordwise location of the elevon hinge line has a large effect on the effectiveness of the elevon (of fixed geometry). The effectiveness of the elevon (when deflected 45°)

for producing pitching moments and for reducing the variation of aerodynamic center with lift was greater with the elevon hinge line on the wing trailing edge than on the 70-percent-chord line. This effect of hinge-line location on flap effectiveness was also shown in reference 4 from tests of a split flap on the inner 0.5 semispan of the untwisted and uncambered 63° swept wing.

A leading-edge flap over the outer 0.22 semispan of the wing sufficiently increased the lift of these sections to remove the instability of the wing between lift coefficients of 0.4 and 0.6 (fig. 9(c)). The stability of the wing above a lift coefficient of 0.4 was further increased by the addition of a 0.5-chord fence at 0.6 semispan on the wing with the leading-edge flap. This resulted in the wing being stable to a lift coefficient of 0.7 with, however, a change of stability between lift coefficients of 0.4 and 0.5.

Adding a spoiler to the inner 0.37 semispan of the wing (fig. 5) to reduce the lift on these sections did not result in any improvement of stability characteristics as shown in figure 9(d). The failure of an improvement of stability to be realized was probably a result of increased spanwise flow from the sections influenced by the spoiler. This spanwise flow also may have kept the spoiler from reducing the lift of the inner portion of the wing span. Adding a fence to the wing near the outer end of the spoiler to reduce this spanwise flow resulted in only small improvements in the effectiveness of the spoiler.

Pressure-Distribution Measurements

Pressure distributions measured at four spanwise stations on the wing are presented in figures 10 and 11, respectively, for the wing alone and for the wing with the fuselage. Data are presented only for the range of lift coefficients wherein large stability changes occurred (lift coefficients from 0.4 to 0.75). The variations of section lift coefficient (obtained from integrated pressure distributions) with wing reference plane angle of attack for a larger lift-coefficient range are shown in figure 12. Included in figure 12 are the variations with angle of attack of pitching-moment coefficient obtained from force tests.

Comparisons of the data of figures 10, 11, and 12 with similar data of reference 7 on the original wing show that the increased thickness and the change of twist of the outer half of the wing resulted in only small changes of the chordwise distributions of pressure and lift of the wing sections. Compared with the pressure distributions on the same sections of the original wing at the same angles of attack (reference 7), the pressure coefficients on the revised wing were less negative on the leading edge near the tip (below the angle of attack for section maximum lift coefficient).

These changes in the pressure distributions on the tip sections did not alter the span load distributions sufficiently to affect noticeably the pressures on the sections at 0.200 and 0.383 semispan. The anticipated increase of maximum lift coefficient of the sections near the tip was not realized.

In reference 7 the variations of stability with lift coefficient of the original wing were attributed principally to variations of span load distribution. The variations of span load distribution were the result of flow separation and the consequent effect on the lift of sections near the tip of the wing. The changes of stability with angle of attack of the revised wing can likewise be attributed to the effects of separation on the spanwise distribution of load.

Although no marked improvements of the stability characteristics were realized from the revised wing, the results of the tests of this wing showed a reduction of the leading-edge pressure peaks near the tip with, however, no resulting improvement of the tip lift characteristics. Thus, the inability of the tip sections of highly swept-back wings to maintain lift to high angles of attack[5] is to a large extent the result of the outward flow of the boundary layer from the root sections rather than local stall of the tip sections.

Thus, improvement of the lift characteristics of the wing sections near the tip by changes of these sections is hindered by the spanwise flow from the root.

Included in figure 12 is the variation of section lift coefficient with angle of attack of the wing with a seal over the gap between the tunnel floor and the model where the base of the model passed through the floor to the model support. In the discussion of the corrections to the data, the effects of this gap on the data obtained on the model were assumed to be small. This assumption is substantiated by the data in figure 12(c) which show a small effect on section lift due to sealing the floor gap.

Span Load Distribution

The modification to the airfoil thickness and twist of the 63° swept wing cambered and twisted for a design lift coefficient of 0.5 (at a Mach number of 1.4) had a negligible effect on the span load distribution as shown by the data in figure 13. Presented in this figure are the basic

[5]This has been shown previously (reference 7) to be the principal cause of the variations of stability with lift on swept-back wings.

(due to twist and camber) and the basic plus the additional[6] (due to angle of attack) span load distributions of the wing without fuselage. Included in this figure is the span load distribution of the revised wing computed by the methods of Weissinger as outlined in references 13 and 14. Reasonably good agreement was obtained between the computed and measured span load distributions.

CONCLUDING REMARKS

The results of tests of a semispan model of a twisted and cambered wing with the leading edge swept back 63° showed that increasing the thickness with a small modification to the twist from midsemispan to the tip resulted in no improvement of the longitudinal characteristics of the wing at low speeds. A reduction in the tip-leading-edge pressure peaks was obtained with no improvement of tip lift characteristics indicating that the early loss of lift of the tip, which resulted in the large variations in longitudinal stability, was due more to spanwise flow of the boundary layer than to local stall of the tip sections.

The change of thickness and twist had a negligible effect on the low-speed drag of the wing.

The addition of stall and boundary-layer-control devices had a considerable effect on the stability of the wing. Upper-surface fences on the inner portion of the wing were nearly as effective as those near the tip for controlling spanwise boundary-layer flow. Fences extending over the after 50 percent of the chord of the wing provided about the same improvement of wing stability as full-chord fences. Addition of a leading-edge flap over the outer 0.22 semispan of the wing with fences at 0.6 and 0.8 semispan resulted in a nearly linear variation of wing pitching-moment coefficient with lift coefficient up to a lift coefficient of 0.7.

Upper-surface split flaps on the outer 0.37 semispan were ineffective for longitudinal control at high lift coefficients but resulted in an approximately linear pitching-moment curve for the wing as a result of the large variation of effectiveness of the split flap with lift coefficient.

---

[6]The basic plus additional load is presented for a lift coefficient ($C_L = 0.4$) at which the local lift and the span loading are not appreciably affected by separation. This lift coefficient corresponds approximately to the low-speed design lift coefficient ($C_L = 0.38$).

The modification of the outer half of the semispan wing resulted in only small changes of the chordwise pressure distributions and lift of the wing sections.

Ames Aeronautical Laboratory,
National Advisory Committee for Aeronautics,
Moffett Field, Calif.

REFERENCES

1. Madden, Robert T.: Aerodynamic Study of a Wing–Fuselage Combination Employing a Wing Swept Back 63°.– Characteristics at a Mach Number of 1.53 Including Effect of Small Variations of Sweep. NACA RM A8J04, 1949.

2. Mas, Newton A.: Aerodynamic Study of a Wing–Fuselage Combination Employing a Wing Swept Back 63°.– Characteristics for Symmetrical Wing Sections at High Subsonic and Moderate Supersonic Mach Numbers. NACA RM A9E09, 1949.

3. McCormack, Gerald M., and Walling, Walter C.: Aerodynamic Study of a Wing–Fuselage Combination Employing a Wing Swept Back 63°.– Investigation of a Large–Scale Model at Low Speed. NACA RM A8D02, 1949.

4. Hopkins, Edward J.: Aerodynamic Study of a Wing–Fuselage Combination Employing a Wing Swept Back 63°.– Effects of Split Flaps, Elevons, and Leading–Edge Devices at Low Speed. NACA RM A9C21, 1949.

5. Madden, Robert T.: Aerodynamic Study of a Wing–Fuselage Combination Employing a Wing Swept Back 63°.– Investigation at a Mach Number of 1.53 to Determine the Effects of Cambering and Twisting the Wing for Uniform Load at a Lift Coefficient of 0.25. NACA RM A9C07, 1949.

6. Jones, J. Lloyd, and Demele, Fred A.: Aerodynamic Study of a Wing–Fuselage Combination Employing a Wing Swept Back 63°.– Characteristics Throughout the Subsonic Speed Range with the Wing Cambered and Twisted for a Uniform Load at a Lift Coefficient of 0.25. NACA RM A9D25, 1949.

7. Weiberg, James A., and Carel, Hubert C.: Wind–Tunnel Investigation at Low Speed of a Wing Swept Back 63° and Twisted and Cambered for a Uniform Load at a Lift Coefficient of 0.5. NACA RM A50A23, 1950.

8. Swanson, Robert S., and Toll, Thomas A.: Jet-Boundary Corrections for Reflection-Plane Models in Rectangular Wind Tunnels. NACA Rep. 770, 1943.

9. Polhamus, Edward C.: Jet-Boundary-Induced-Upwash Velocities for Swept Reflection-Plane Models Mounted Vertically in 7- by 10-Foot Closed, Rectangular Wind Tunnels. NACA TN 1752, 1948.

10. Graham, Robert R., and Conner, D. William: Investigation of High-Lift and Stall-Control Devices on an NACA 64-Series 42° Swept-back Wing With and Without Fuselage. NACA RM L7G09, 1947.

11. Conner, D. William, and Neely, Robert H.: Effects of a Fuselage and Various High-Lift and Stall-Control Flaps on Aerodynamic Characteristics in Pitch of an NACA 64-Series 40° Swept-Back Wing. NACA RM L6L27, 1947.

12. Jones, Robert T.: Wing Plan Forms for High-Speed Flight. NACA TN 1033, 1946.

13. DeYoung, John: Theoretical Additional Span Loading Characteristics of Wings with Arbitrary Sweep, Aspect Ratio, and Taper Ratio. NACA Rep. 921, 1948.

14. Stevens, Victor I.: Theoretical Basic Span Loading Characteristics of Wings with Arbitrary Sweep, Aspect Ratio, and Taper Ratio. NACA TN 1772, 1948.

TABLE I.- CHORDWISE LOCATIONS OF THE PRESSURE ORIFICES

[Orifices located on both upper and lower wing surfaces]

Percent wing chord	
0	30.00
1.25	40.00
2.50	50.00
5.00	60.00
7.50	70.00
10.00	80.00
15.00	90.00
20.00	95.00
25.00	

TABLE II.- DIMENSIONS OF THE SEMISPAN MODEL

Wing	
Area of semispan model, $\frac{S}{2}$, square feet	14.262[a]
Semispan, feet	5.0
Mean aerodynamic chord, feet	3.20
Aspect ratio	3.5[b]
Taper ratio (ratio of tip chord to root chord)	0.25
Sweepback of leading edge, degrees	63
Sweepback of quarter-chord line, degrees	60.8
Geometric twist, degrees	20.5
Dihedral, degrees	0
Fuselage	
Length, feet	14.2
Maximum diameter, feet	1.36
Fineness ratio (ratio of length to maximum diameter)	10.4

[a]Area to projected tip was 14.286 square feet.

[b]Based on span of 10 feet and area (to projected tip) of 28.572 square feet.

TABLE III.- COORDINATES OF THE FUSELAGE

[All dimensions in inches]

Station	Diameter	Station	Diameter
0	0	81.6	16.32
4	2.84	91.8	16.20
8	5.34	102.0	15.82
12	7.50	112.2	15.20
16	9.30	122.4	14.28
20	10.80	132.6	13.26
24	11.98	142.8	11.68
28	12.88	153.0	9.86
30.6	13.26	163.2	7.58
40.8	14.28	164.4	7.16
51.0	15.20	166.4	5.82
61.2	15.82	168.4	3.58
71.4	16.20	170.4	0

Fineness ratio, $\frac{\text{length}}{\text{maximum diameter}} = 10.4$

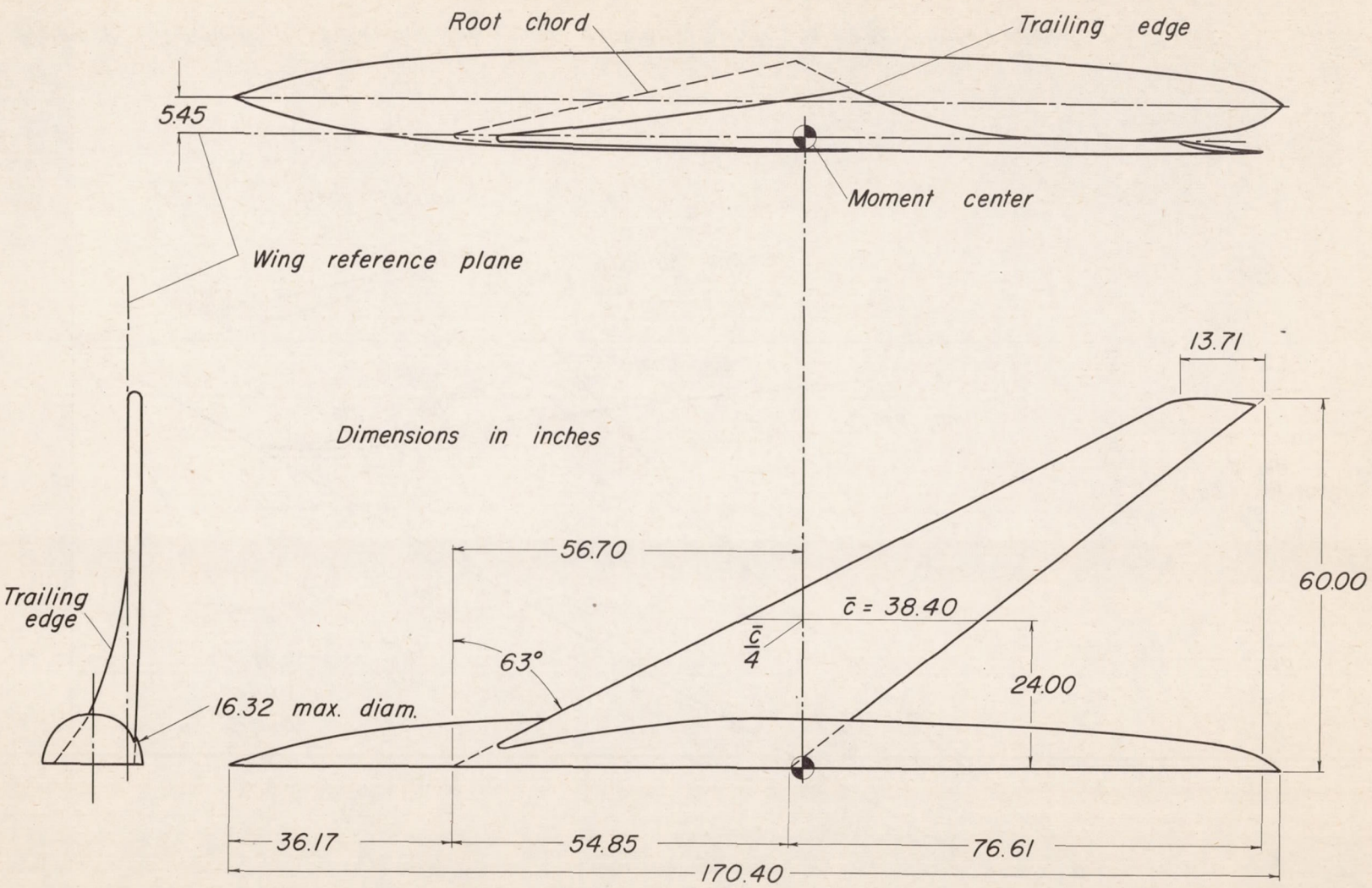

Figure 1.- Diagram of the model.

CONFIDENTIAL

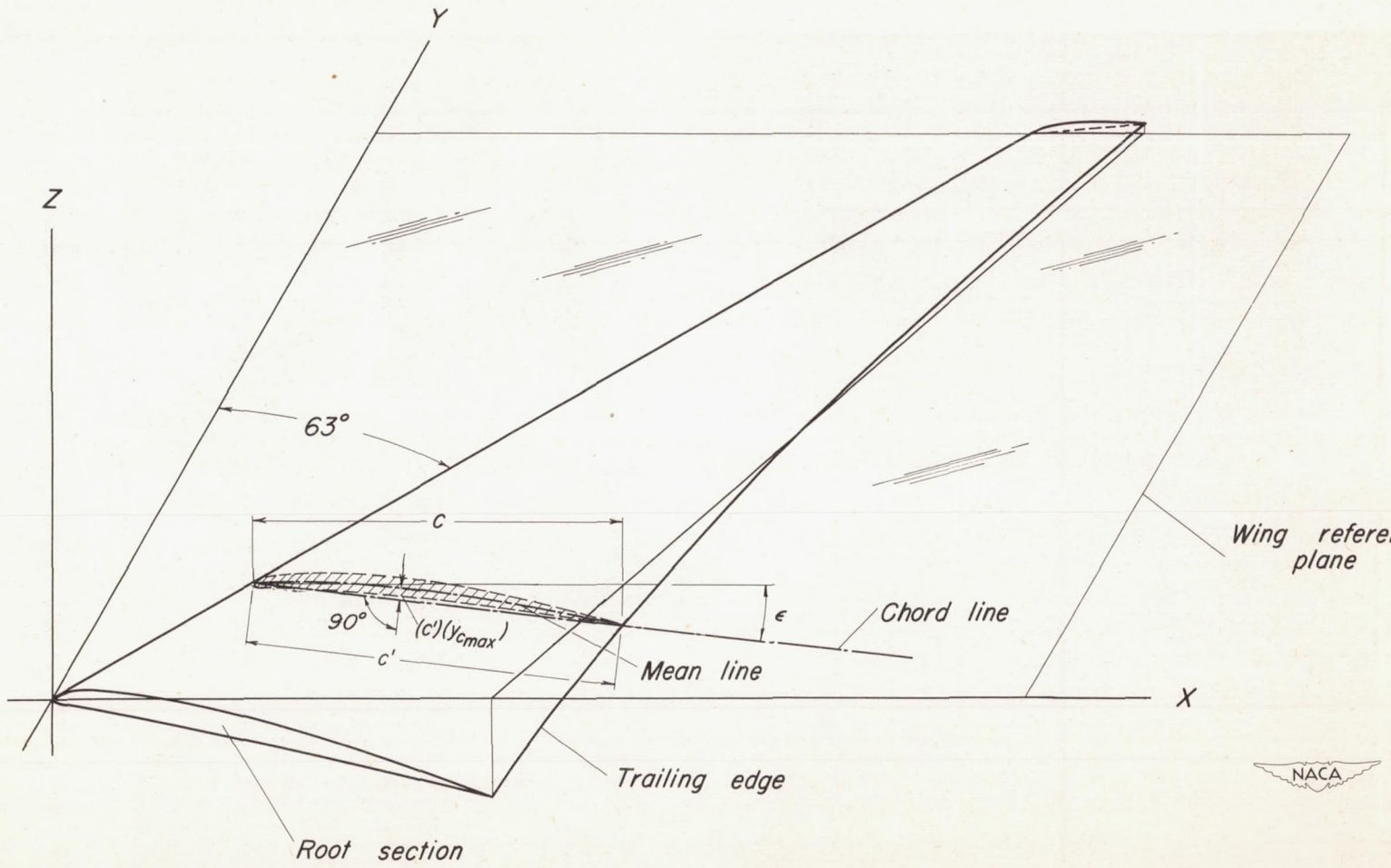

Figure 2.— Relationship between the wing geometry and the coordinate axes.

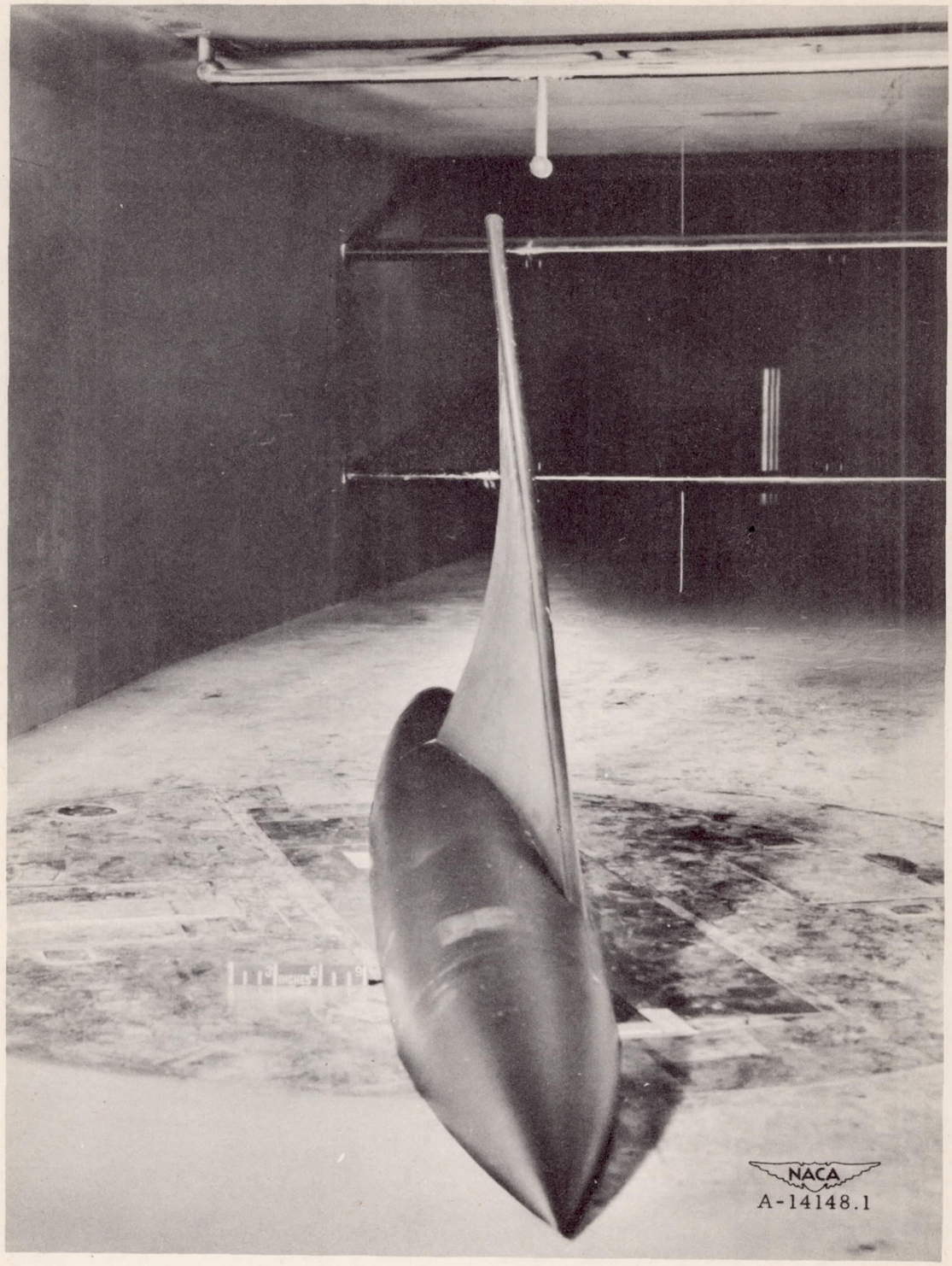

Figure 3.- The model mounted in the wind tunnel.

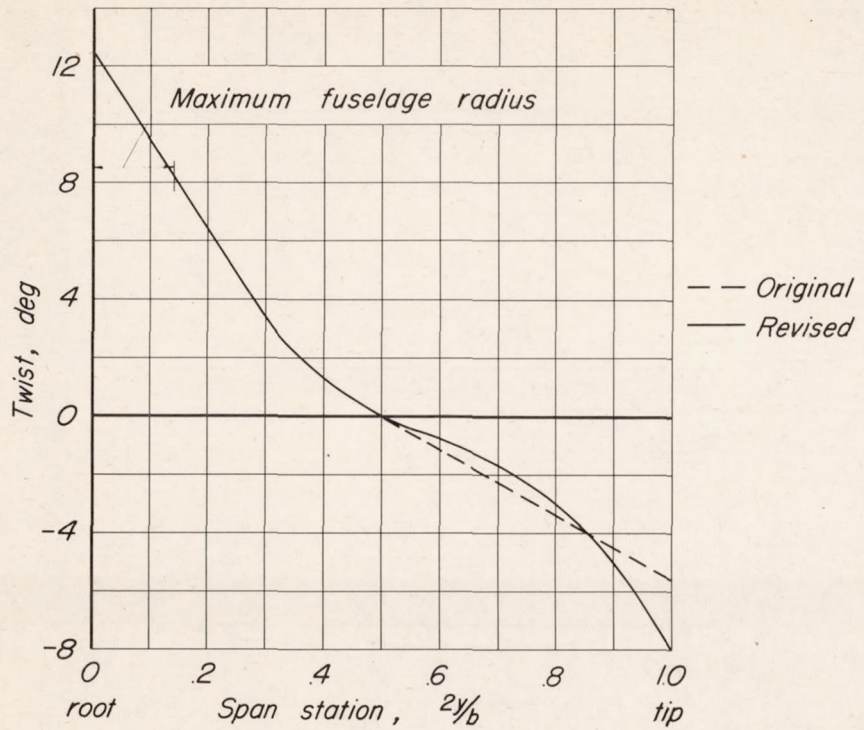

(a) Twist.

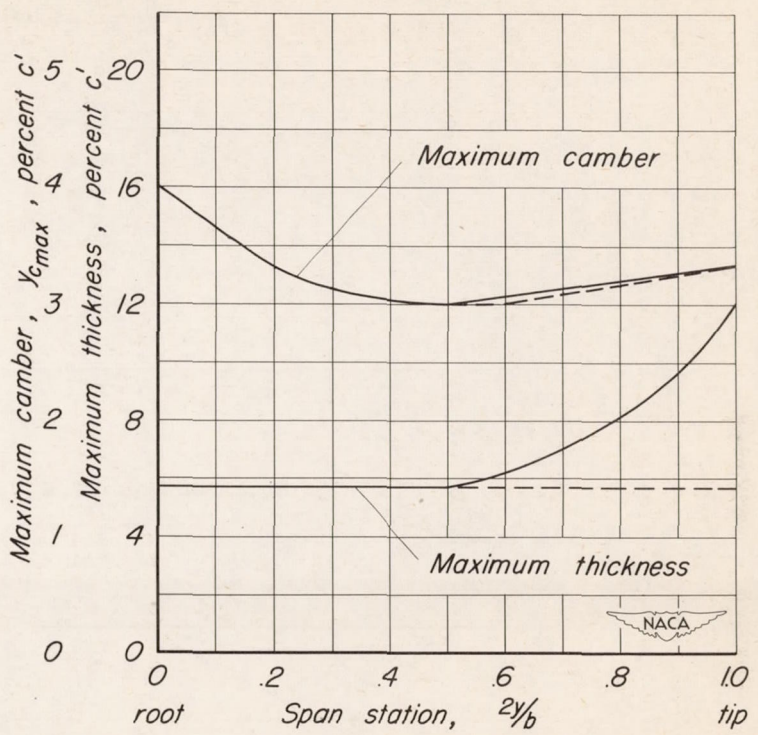

(b) Maximum camber and maximum thickness.

Figure 4.- Comparison of original and revised twist, maximum camber, and maximum thickness.

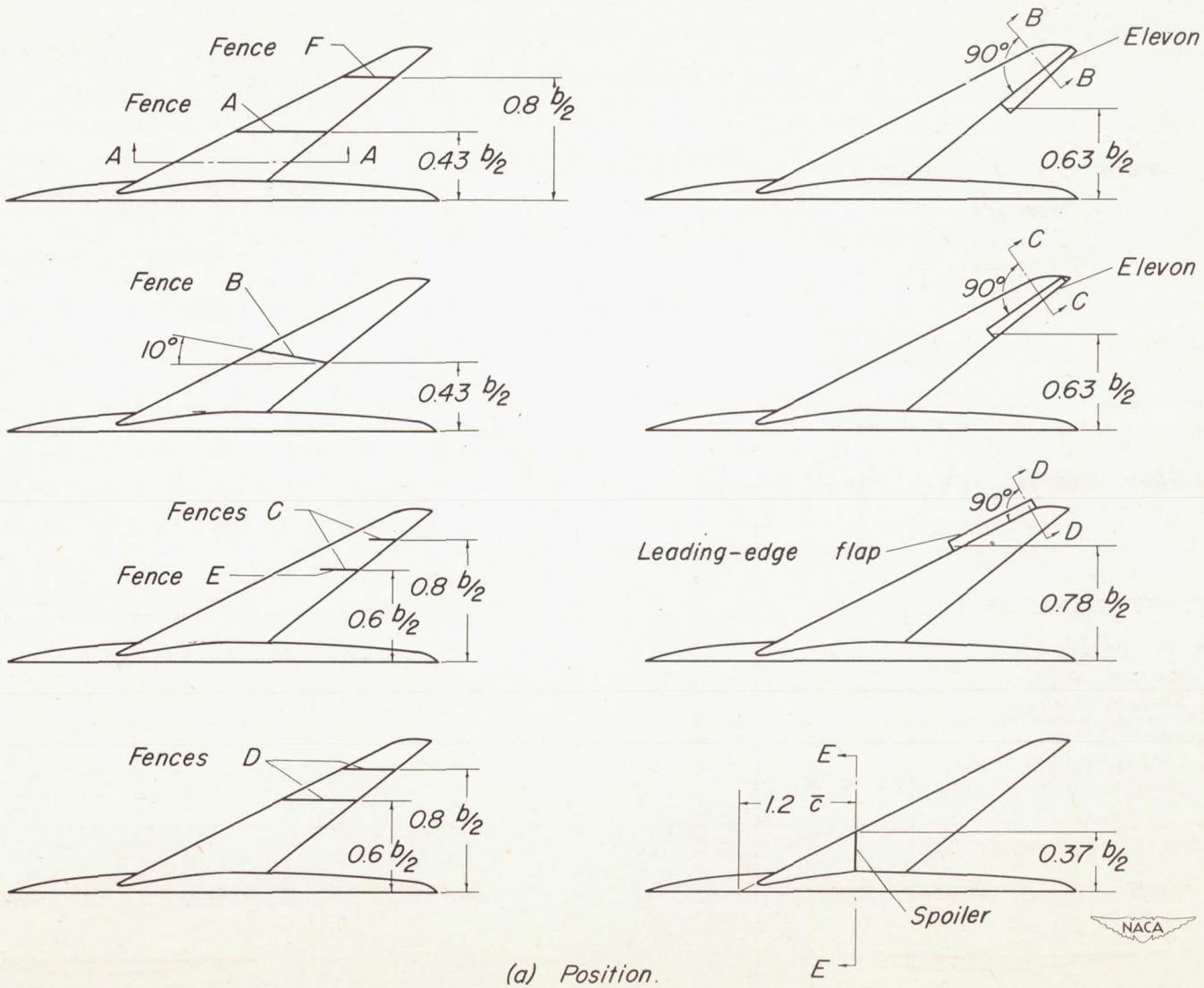

(a) Position.

Figure 5.- Geometry of the stall-control devices.

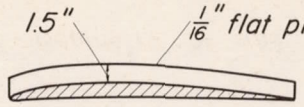

Typical section A - A, fences A, B, D, and F

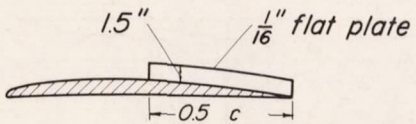

Typical section A - A, fences C and E

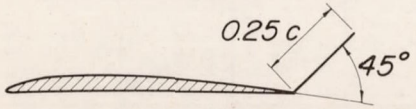

Typical section B - B, elevon 1

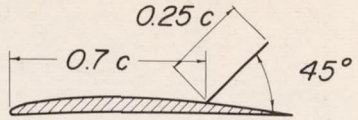

Typical section C - C, elevon 2

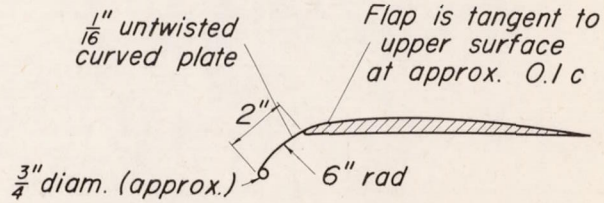

Typical section D - D, leading - edge flap

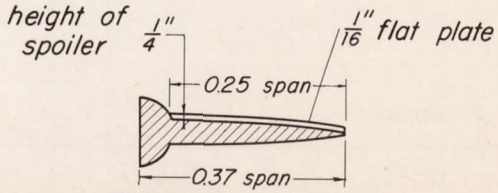

Section E - E, spoiler

(b) Dimensions.

Figure 5.- Concluded.

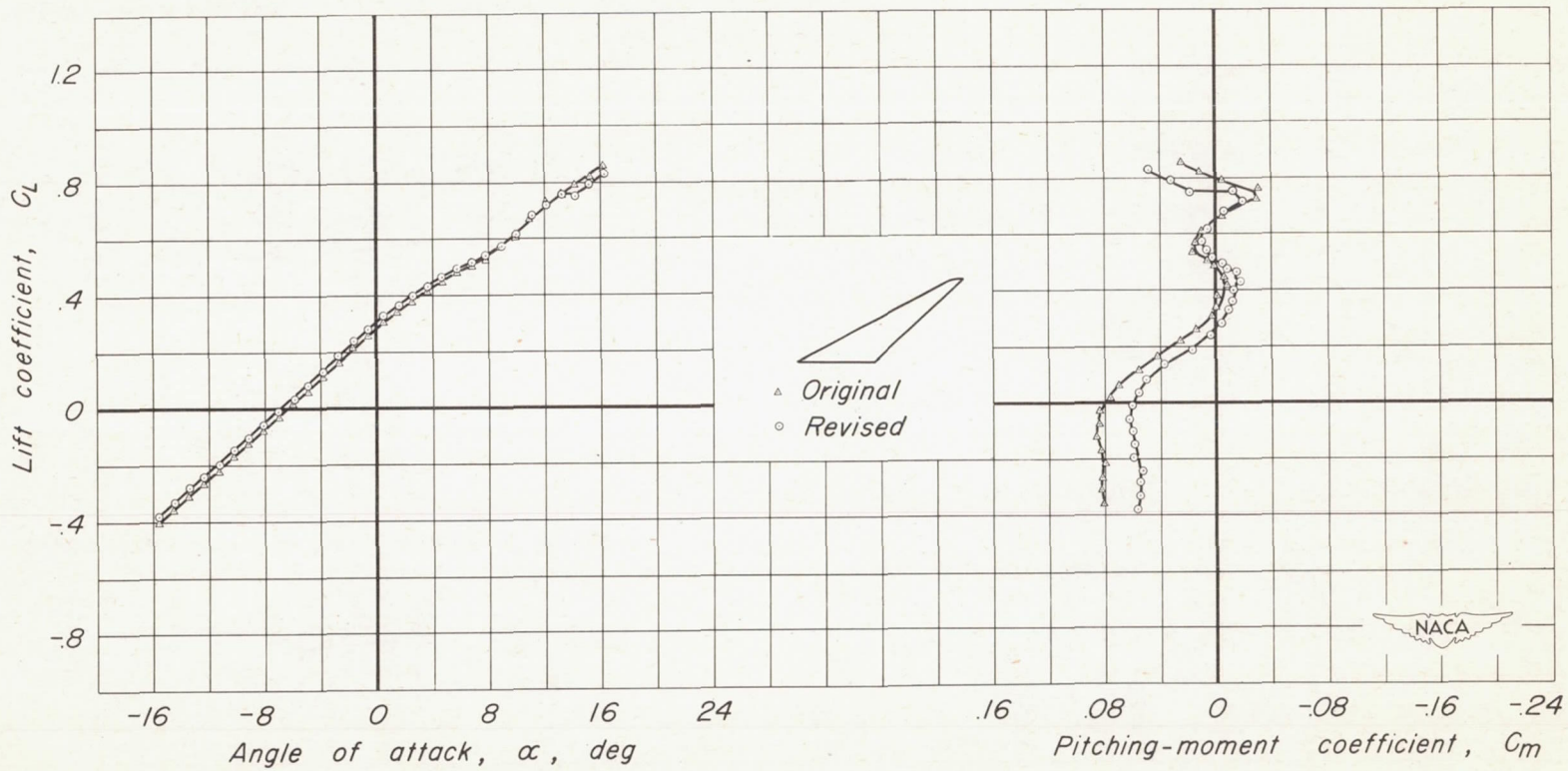

(a) Wing.

Figure 6.- Effect of wing revision on the lift and pitching-moment characteristics.

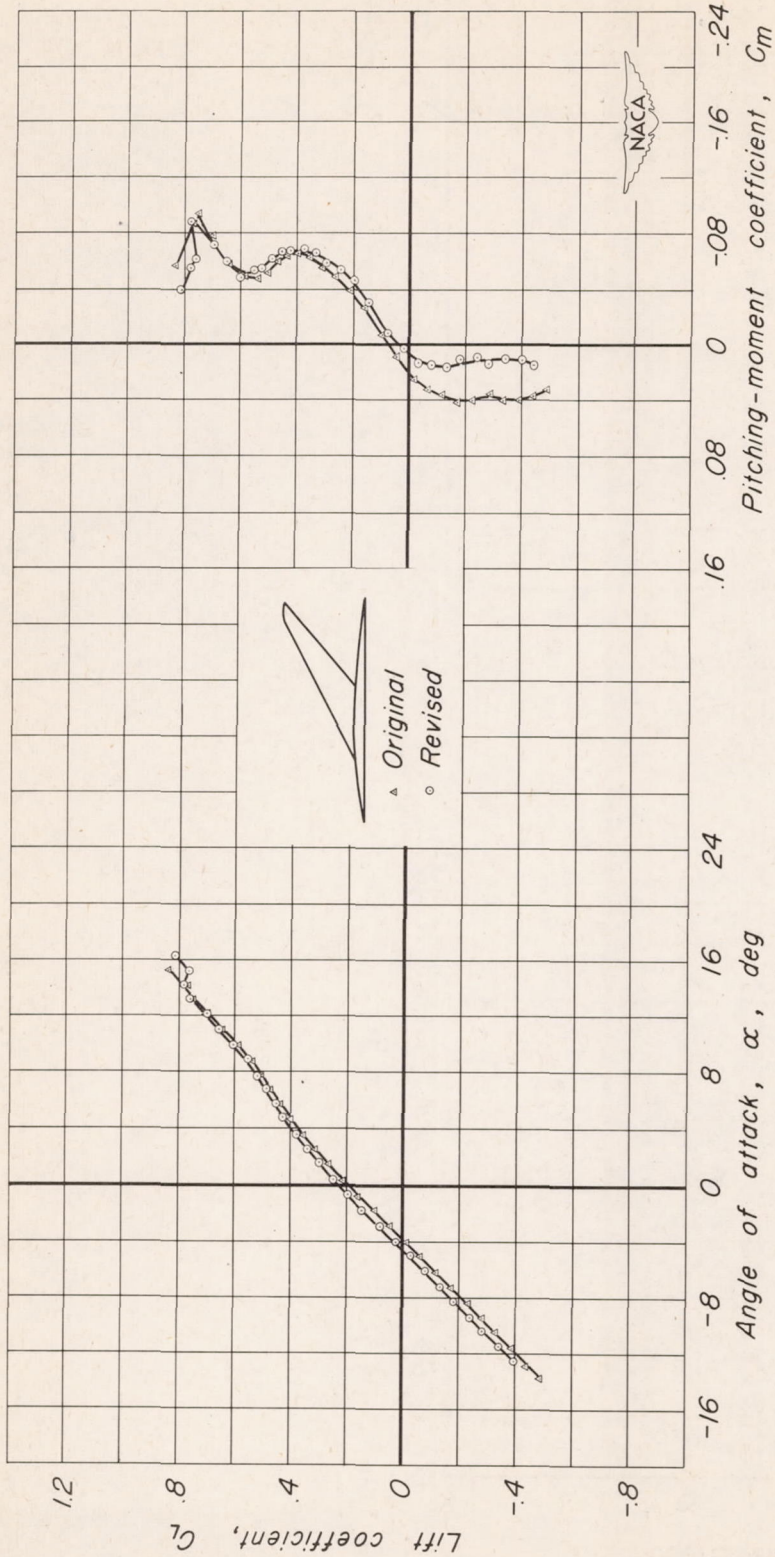

(b) Wing with fuselage.

Figure 6.-Concluded.

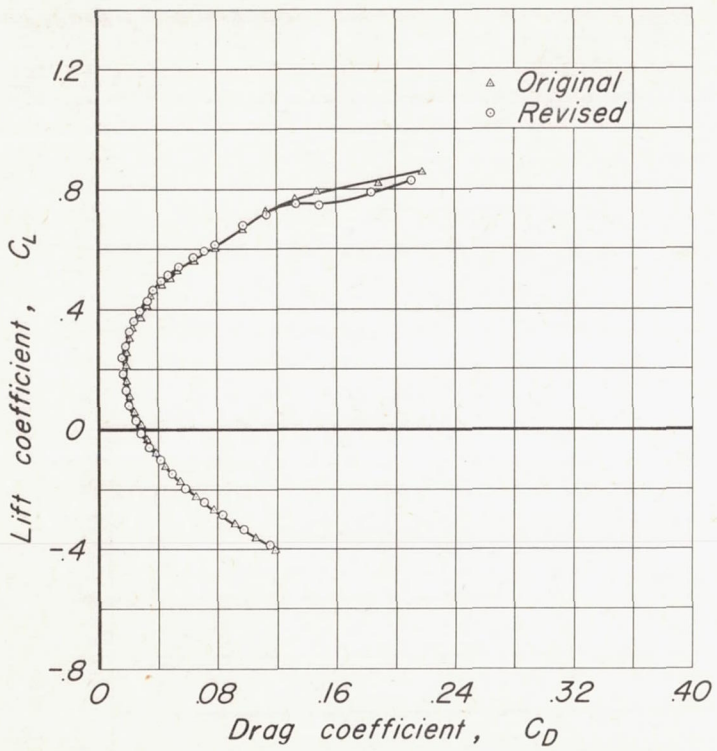

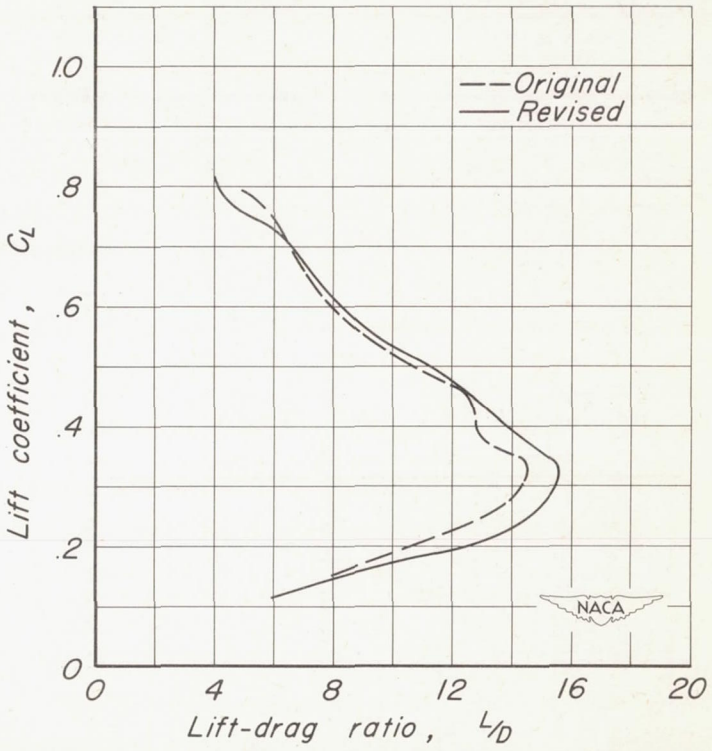

(a)Wing.

Figure 7.-Effect of wing revision on the drag and lift-drag ratio.

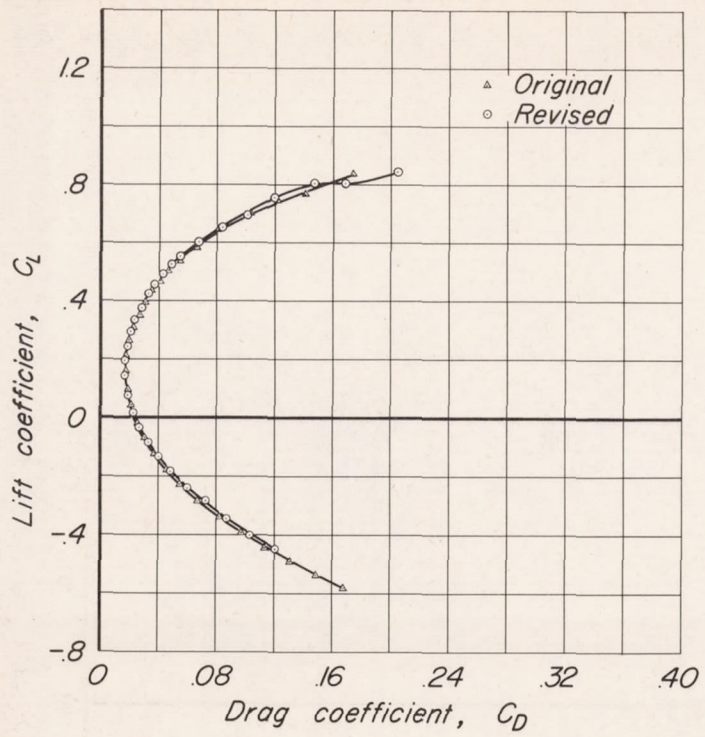

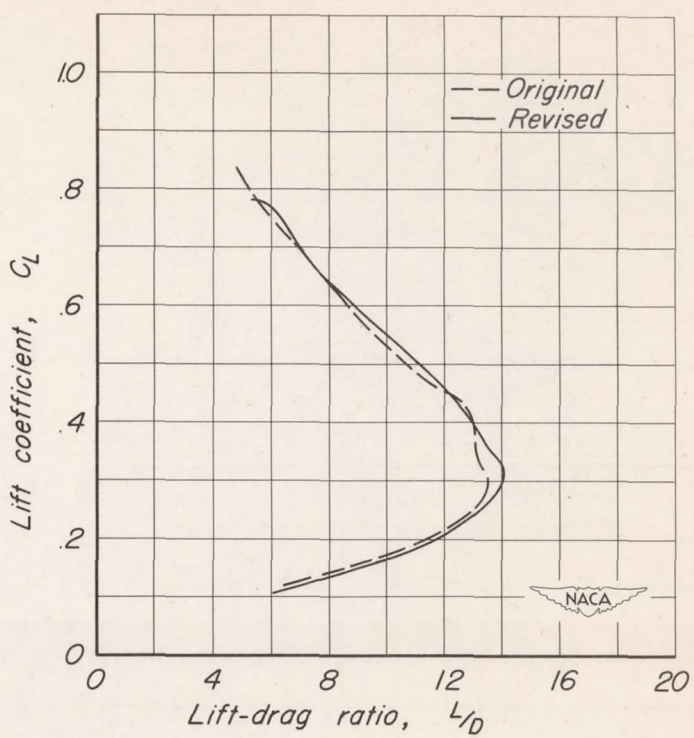

(b) Wing with fuselage.

Figure 7.- Concluded.

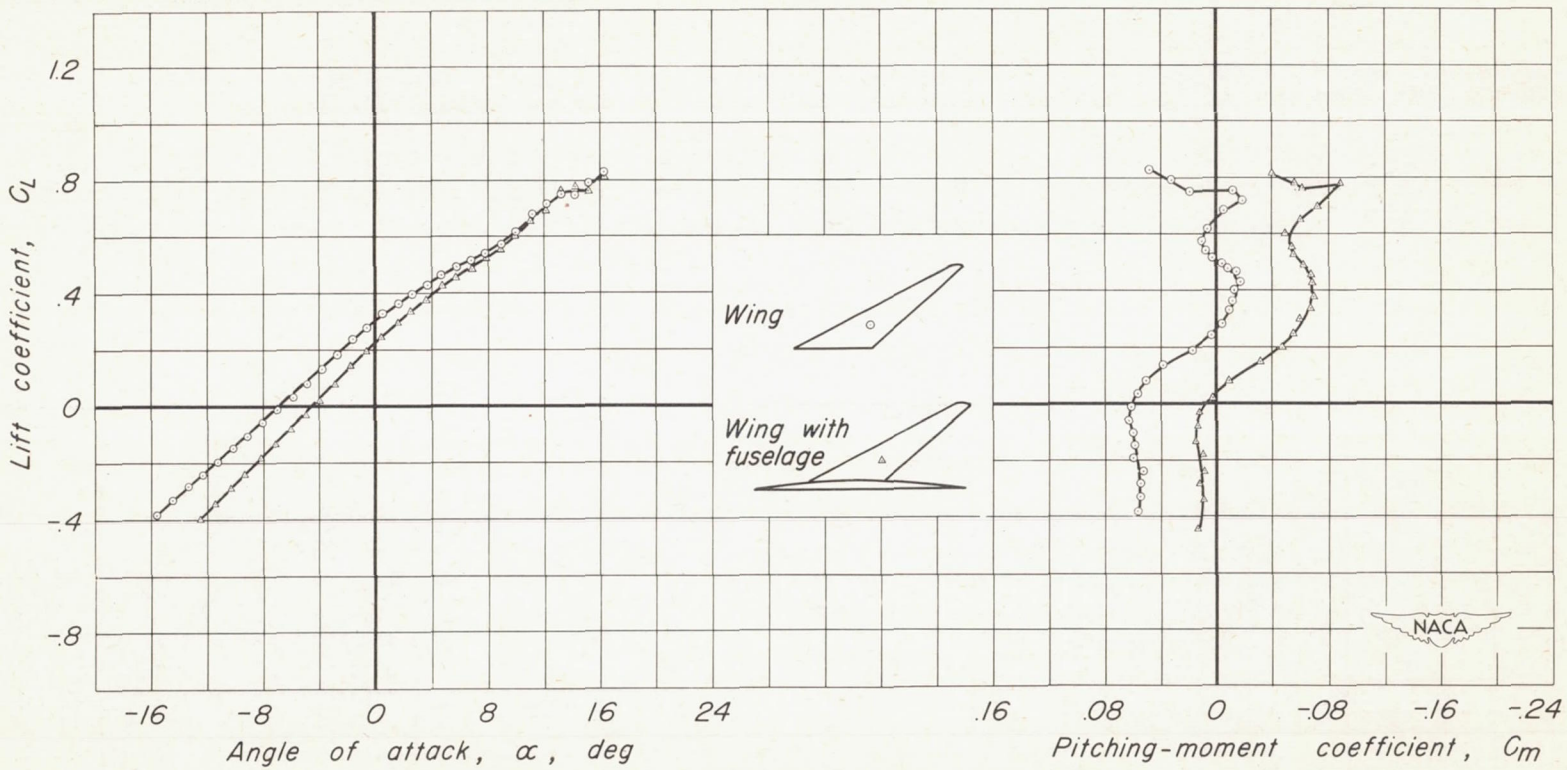

Figure 8.-Effect of a fuselage on the lift and pitching-moment characteristics.

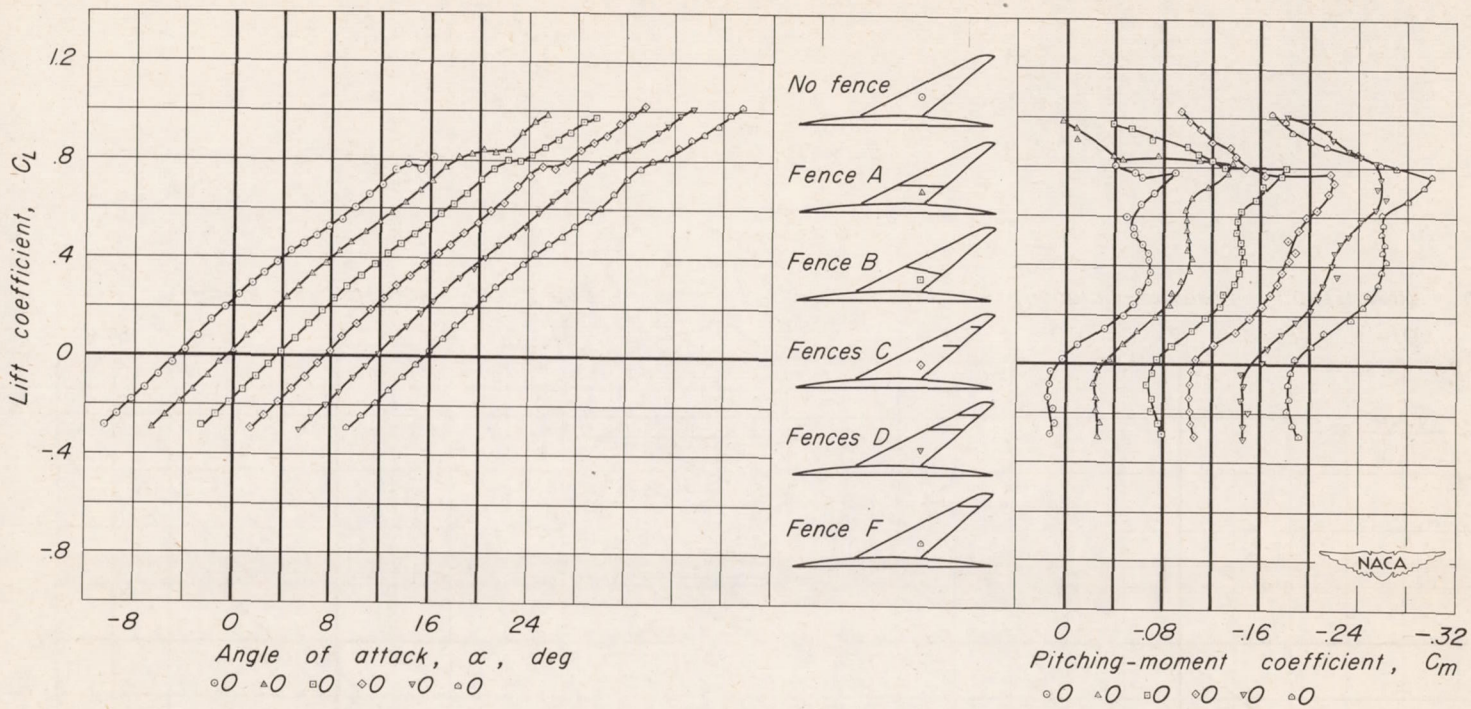

(a) Fences.

Figure 9.-Effect of stall-control devices on the lift and pitching-moment characteristics of the wing with fuselage.

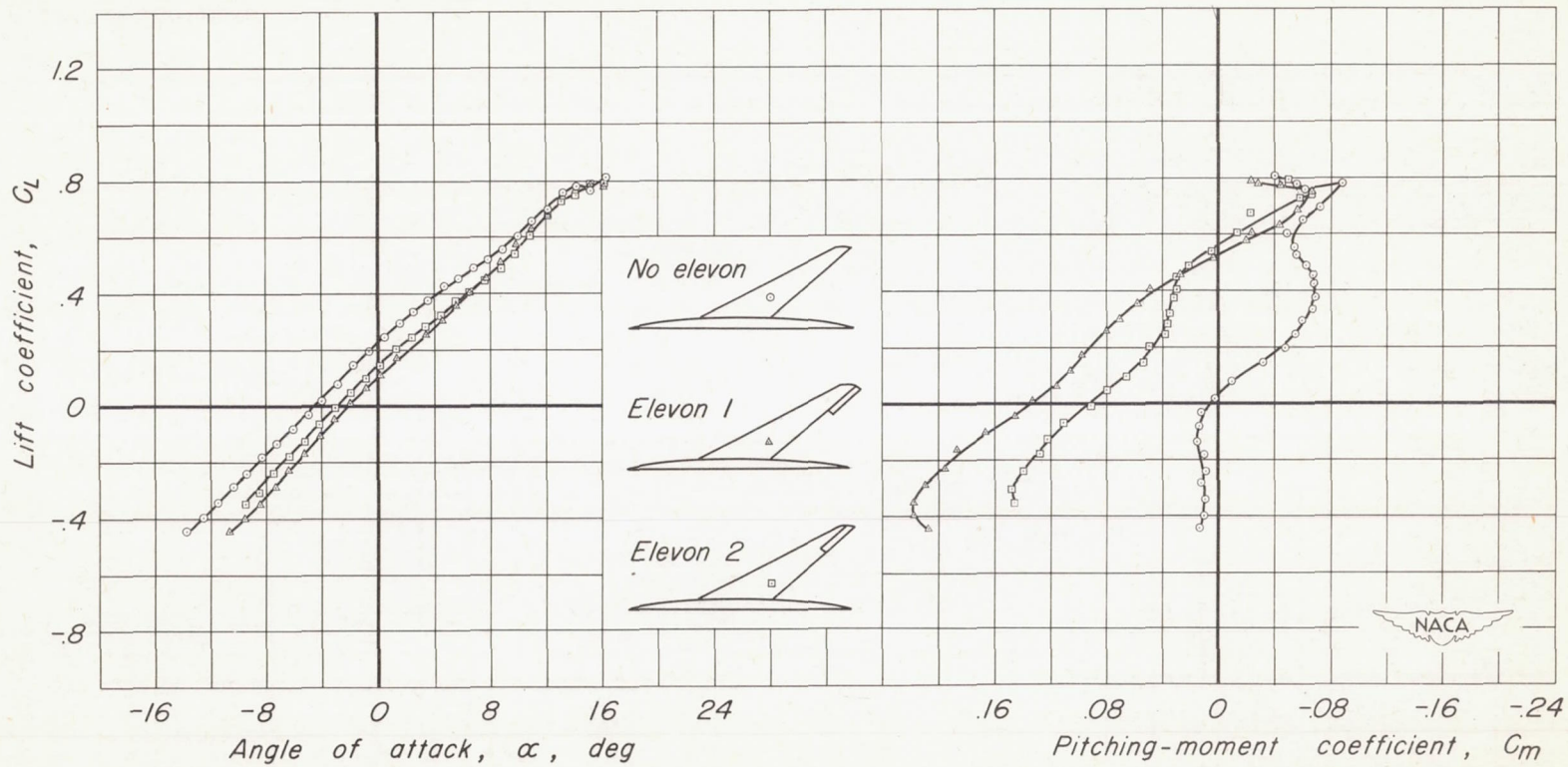

(b) Elevon.

Figure 9.-Continued.

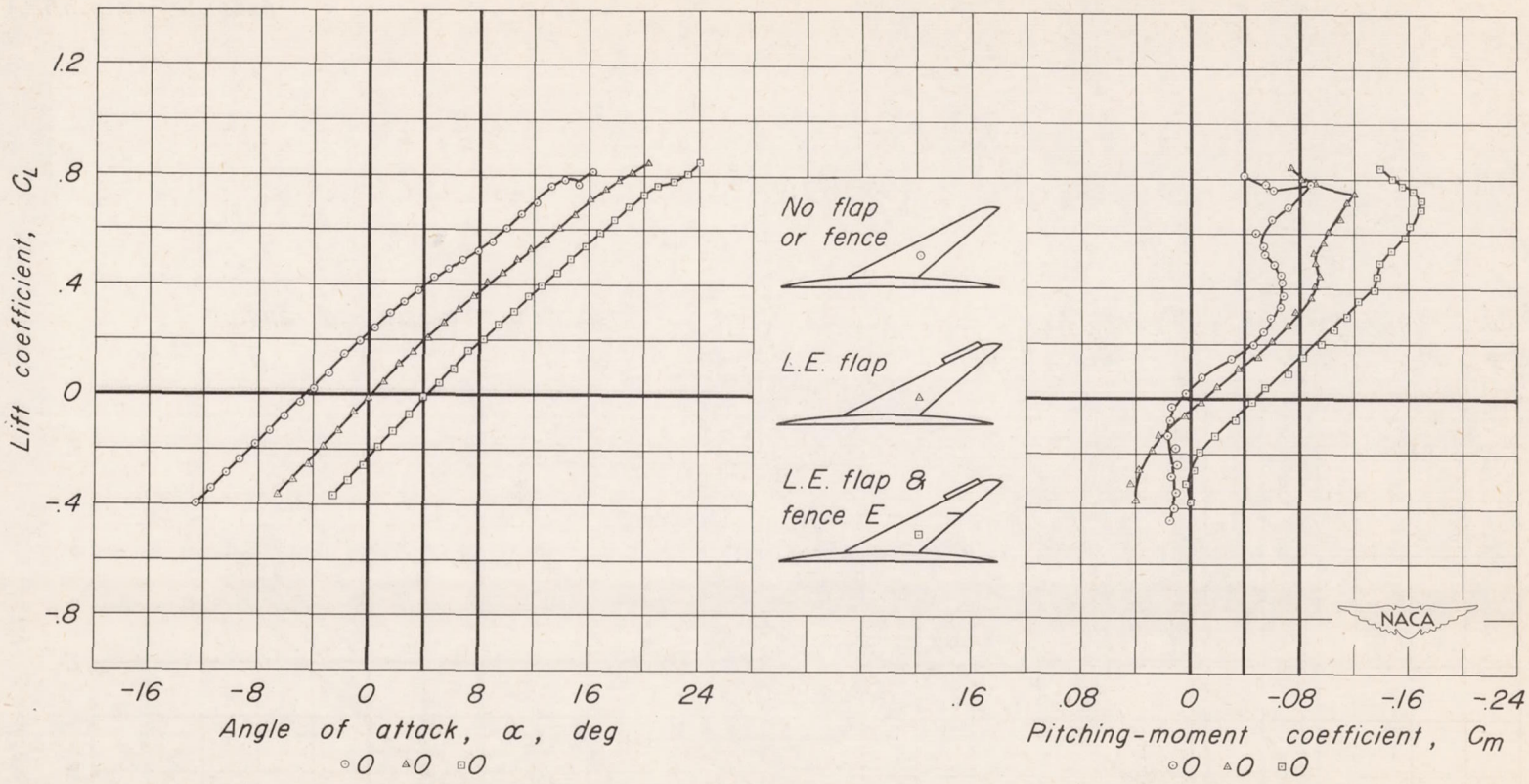

(c) Leading-edge flap.

Figure 9.-Continued.

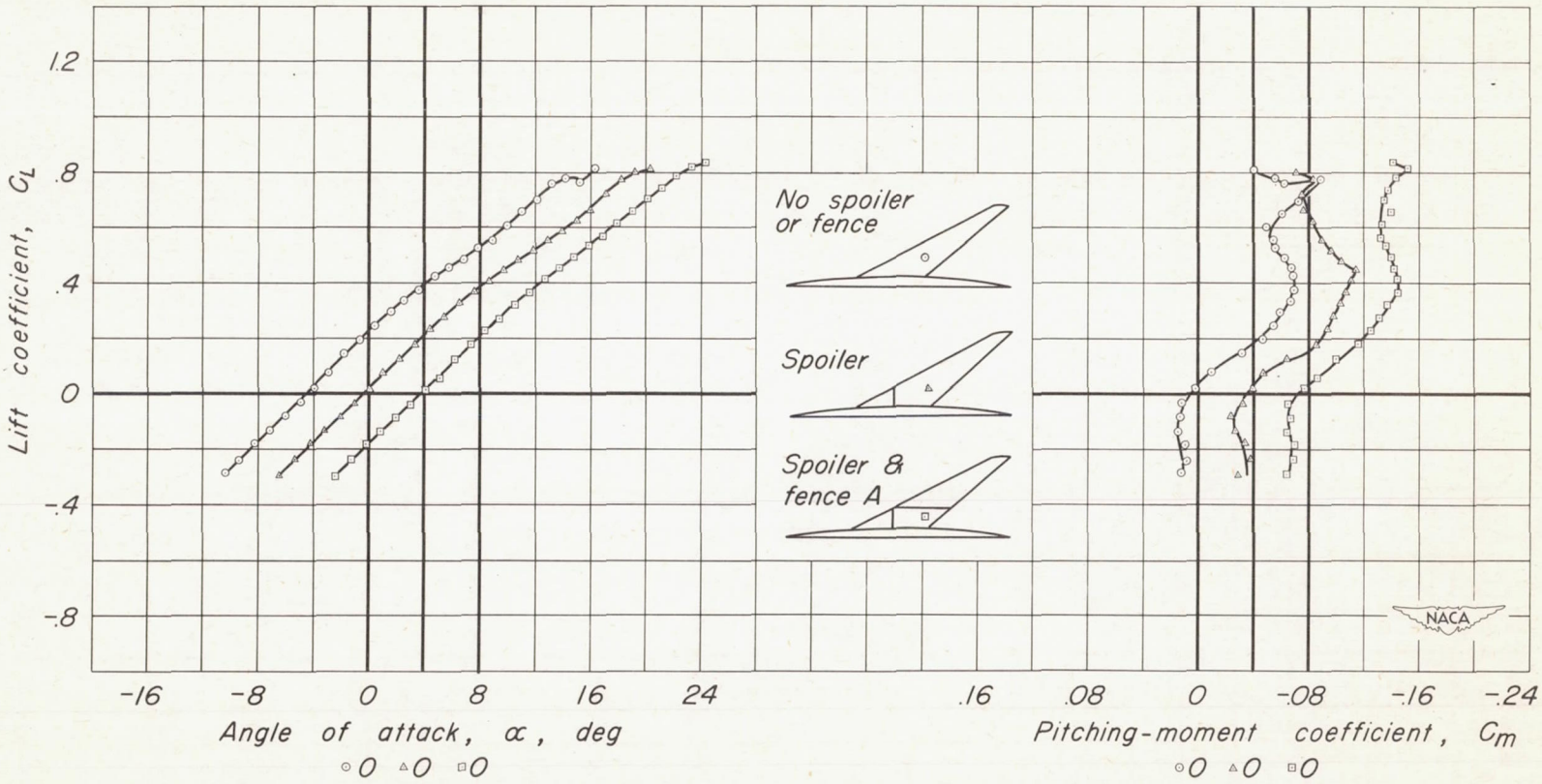

(d) Spoiler.

Figure 9.-Concluded.

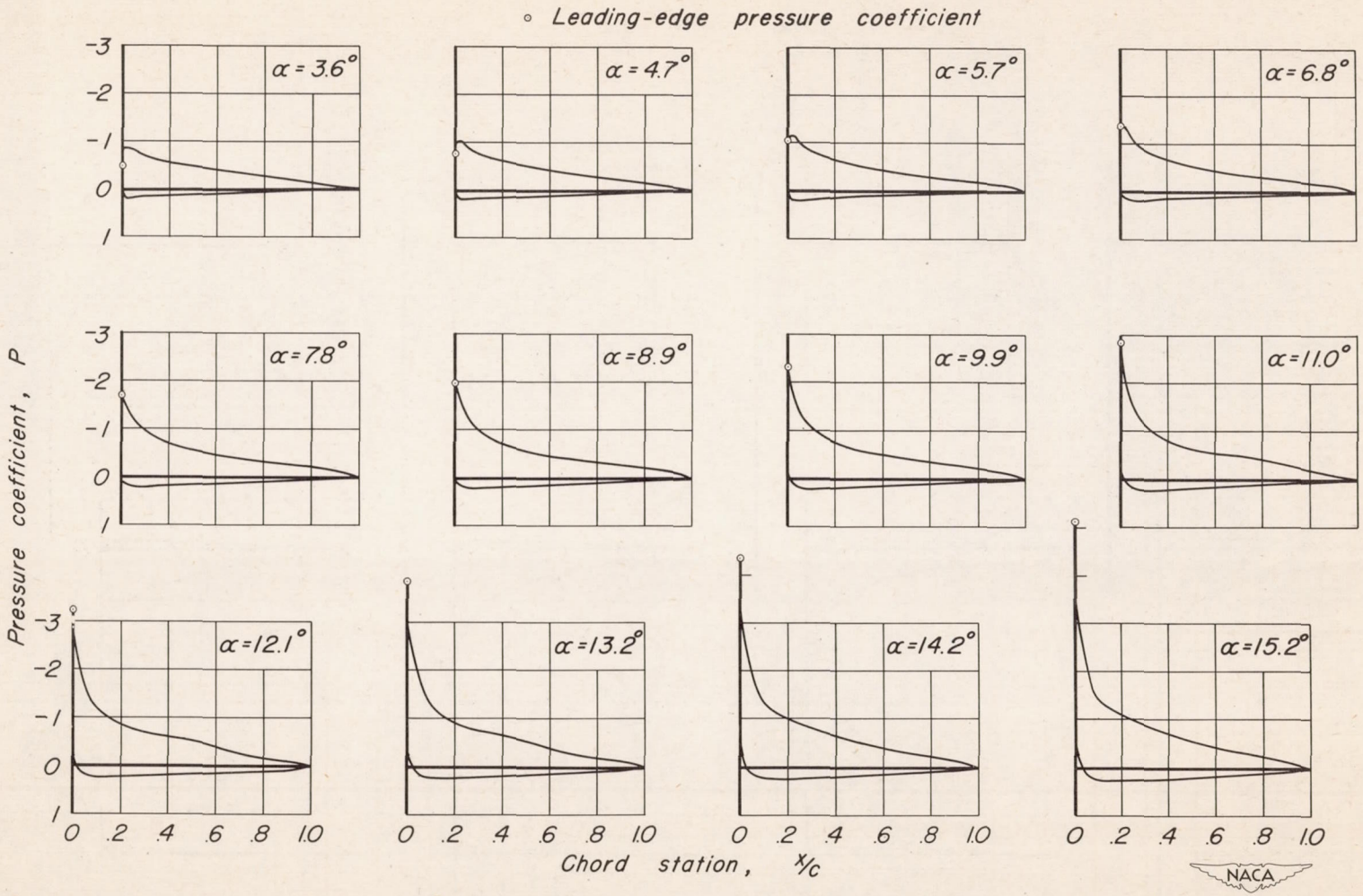

(a) 0.200 semispan.

Figure 10.- Pressure distribution on the wing.

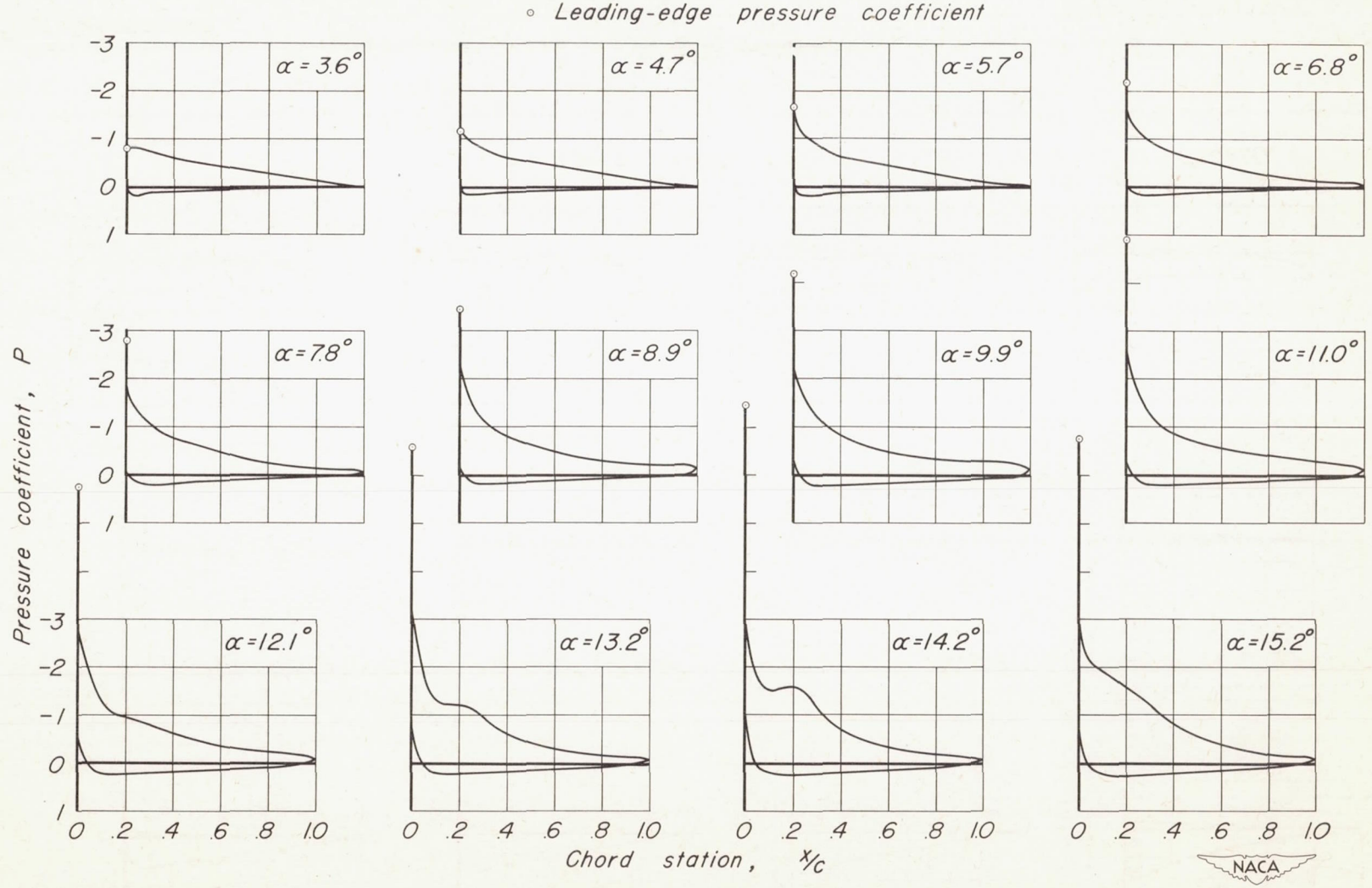

(b) 0.383 semispan.

Figure 10.- Continued.

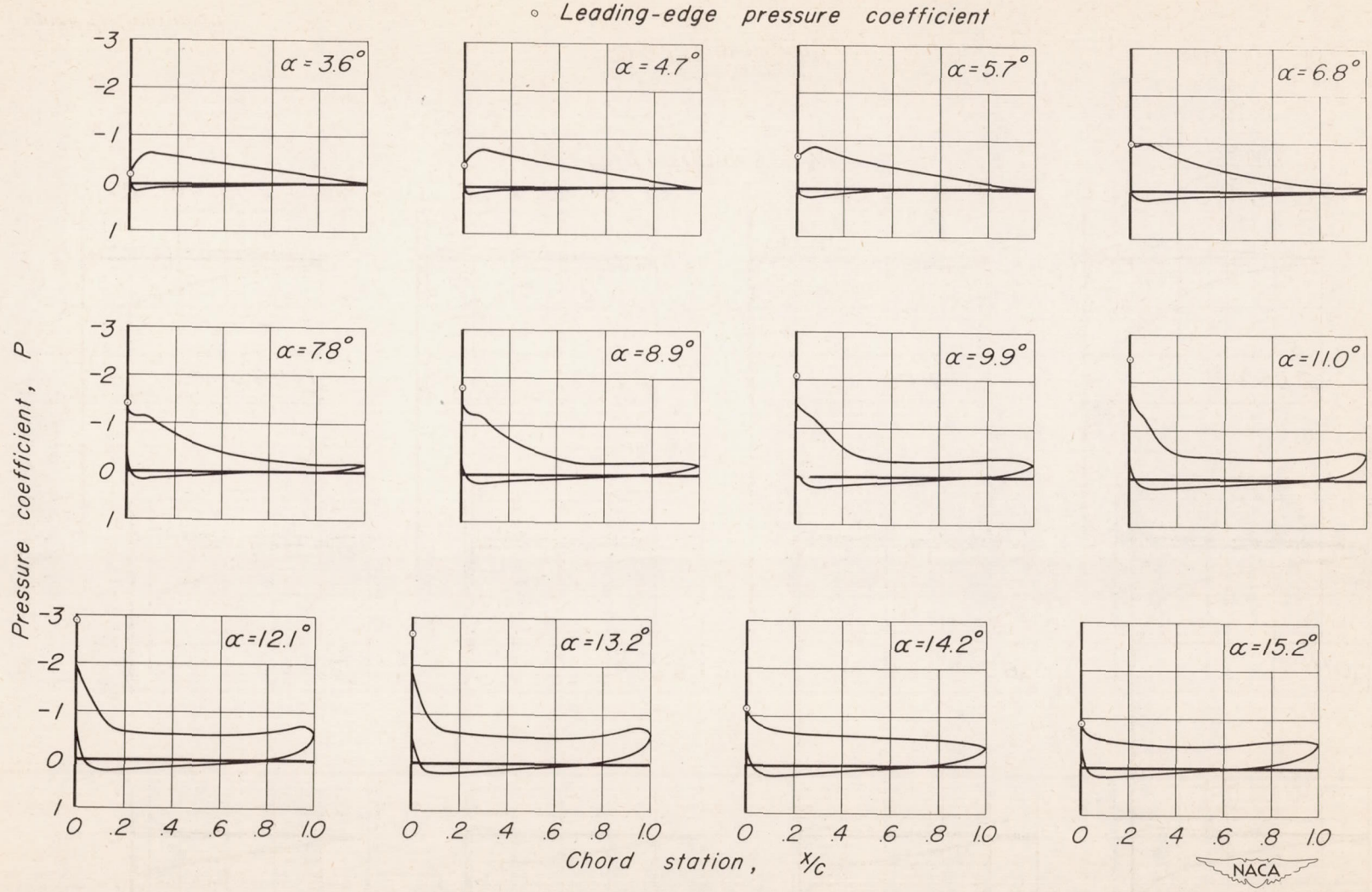

(c) 0.707 semispan.

Figure10-Continued.

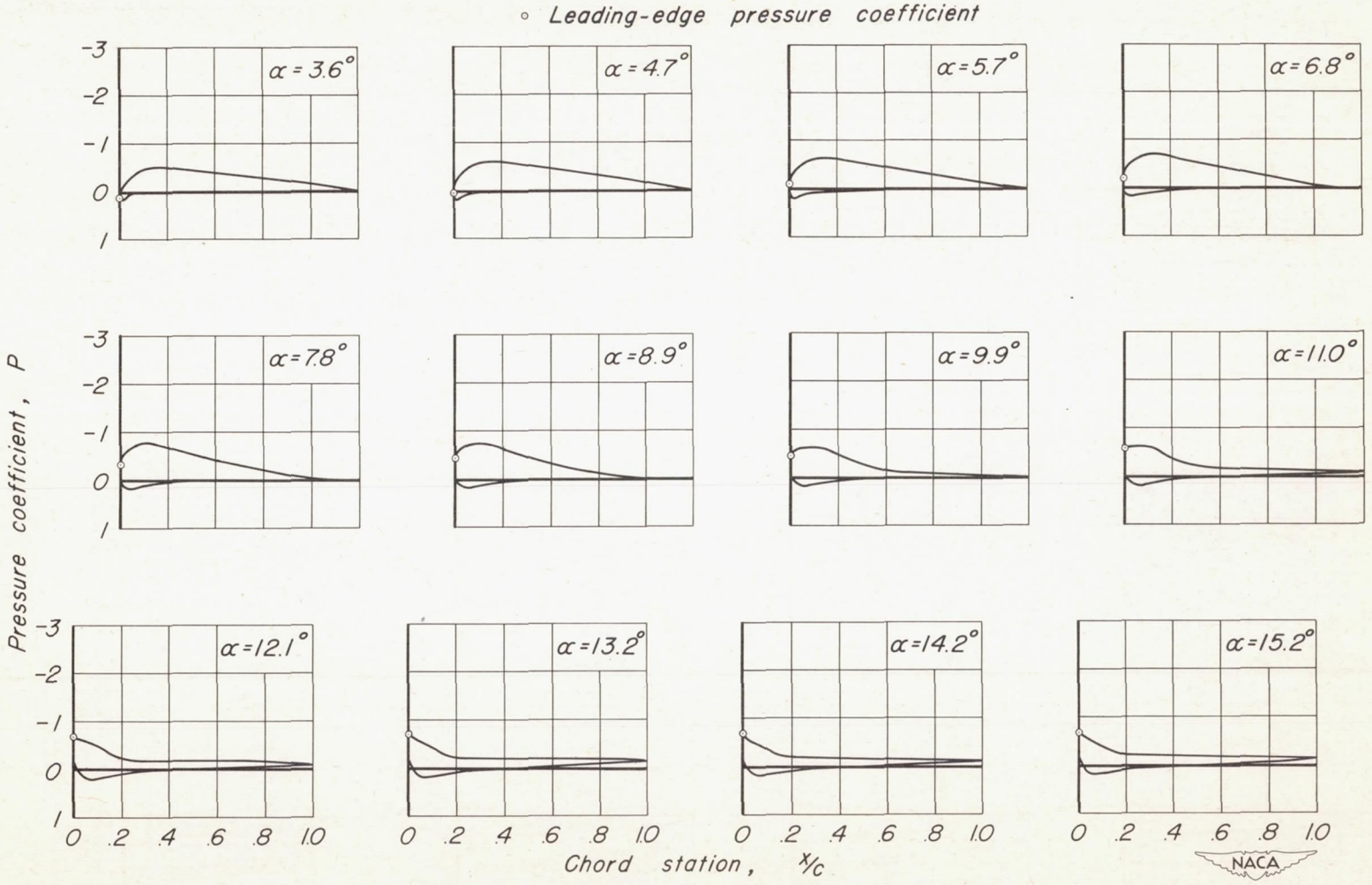

(d) 0.924 semispan.

Figure 10.- Concluded.

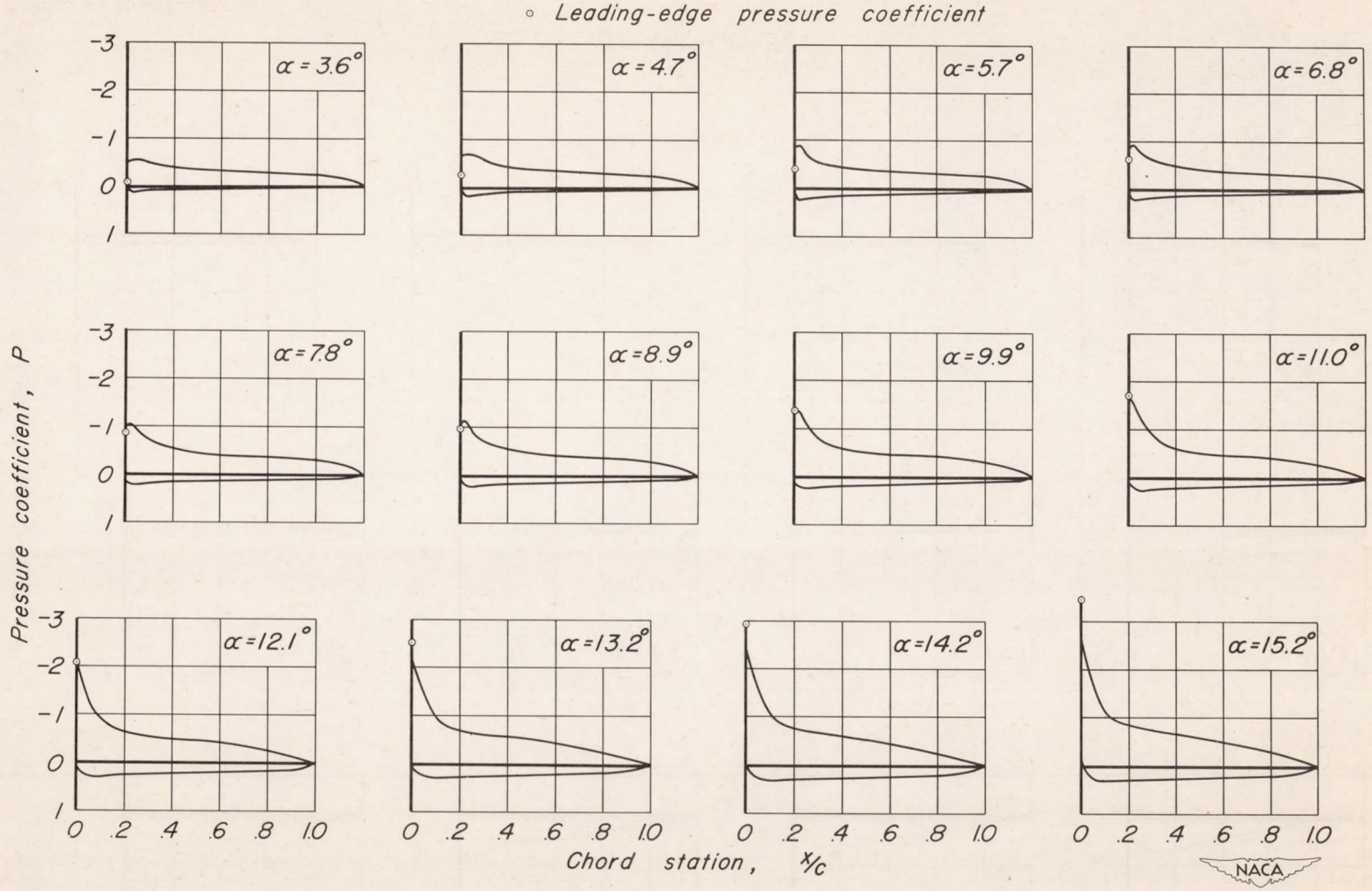

(a) 0.200 semispan.

Figure 11.-Pressure distribution on the wing with fuselage.

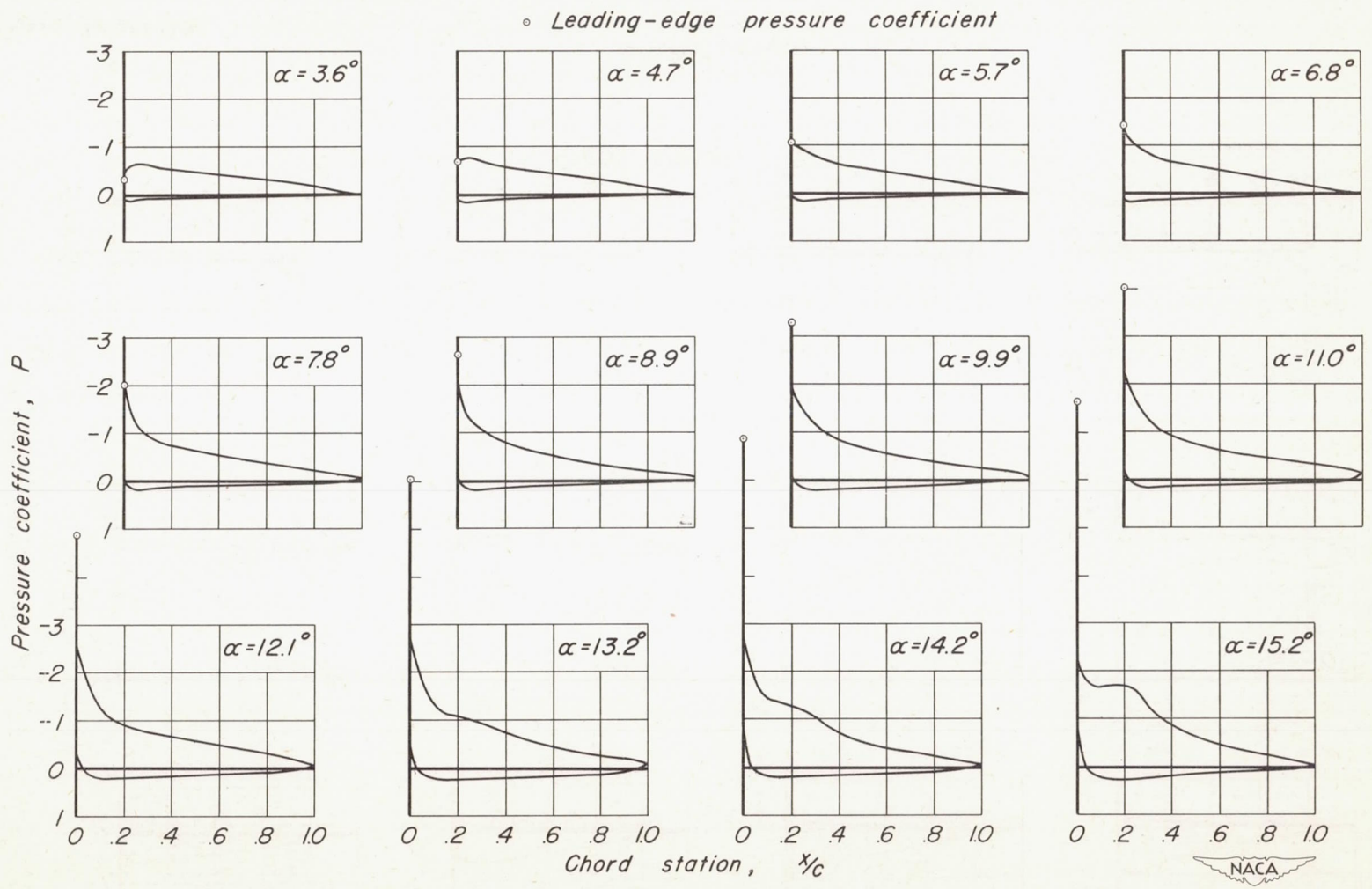

(b) 0.383 semispan.

Figure 11.-Continued.

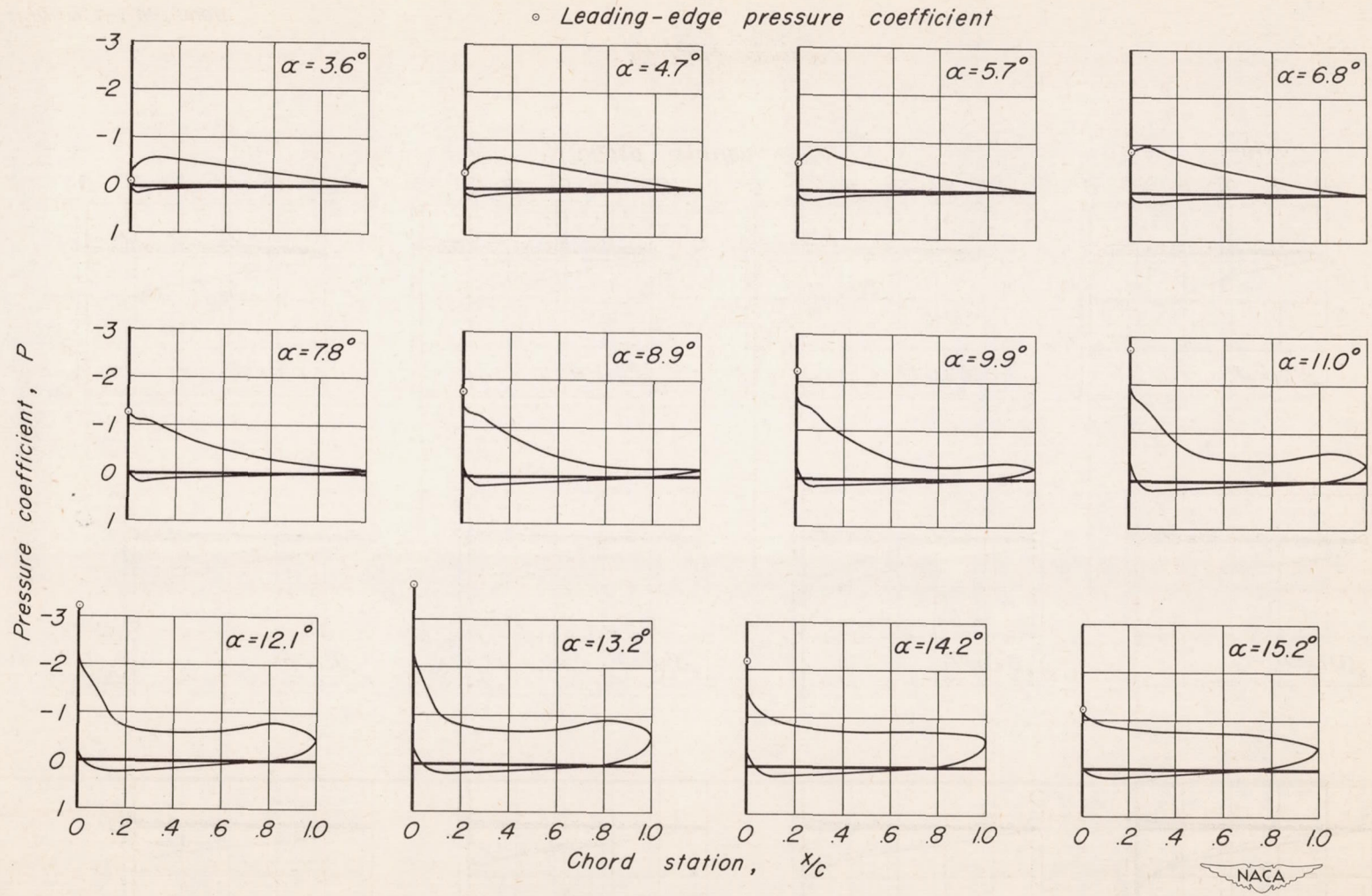

(c) 0.707 semispan.

Figure 11-Continued.

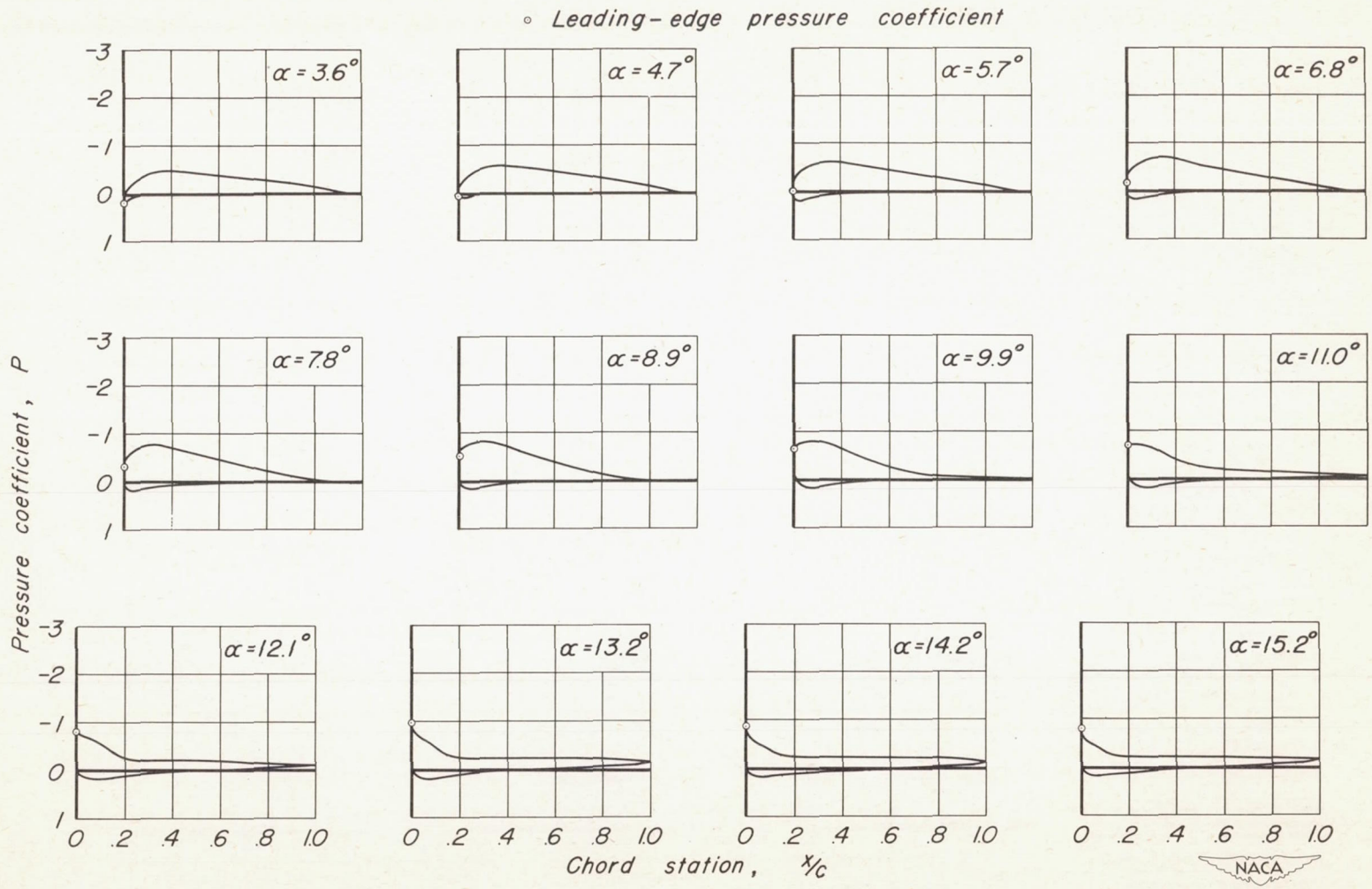

(d) 0.924 semispan.

Figure 11.-Concluded.

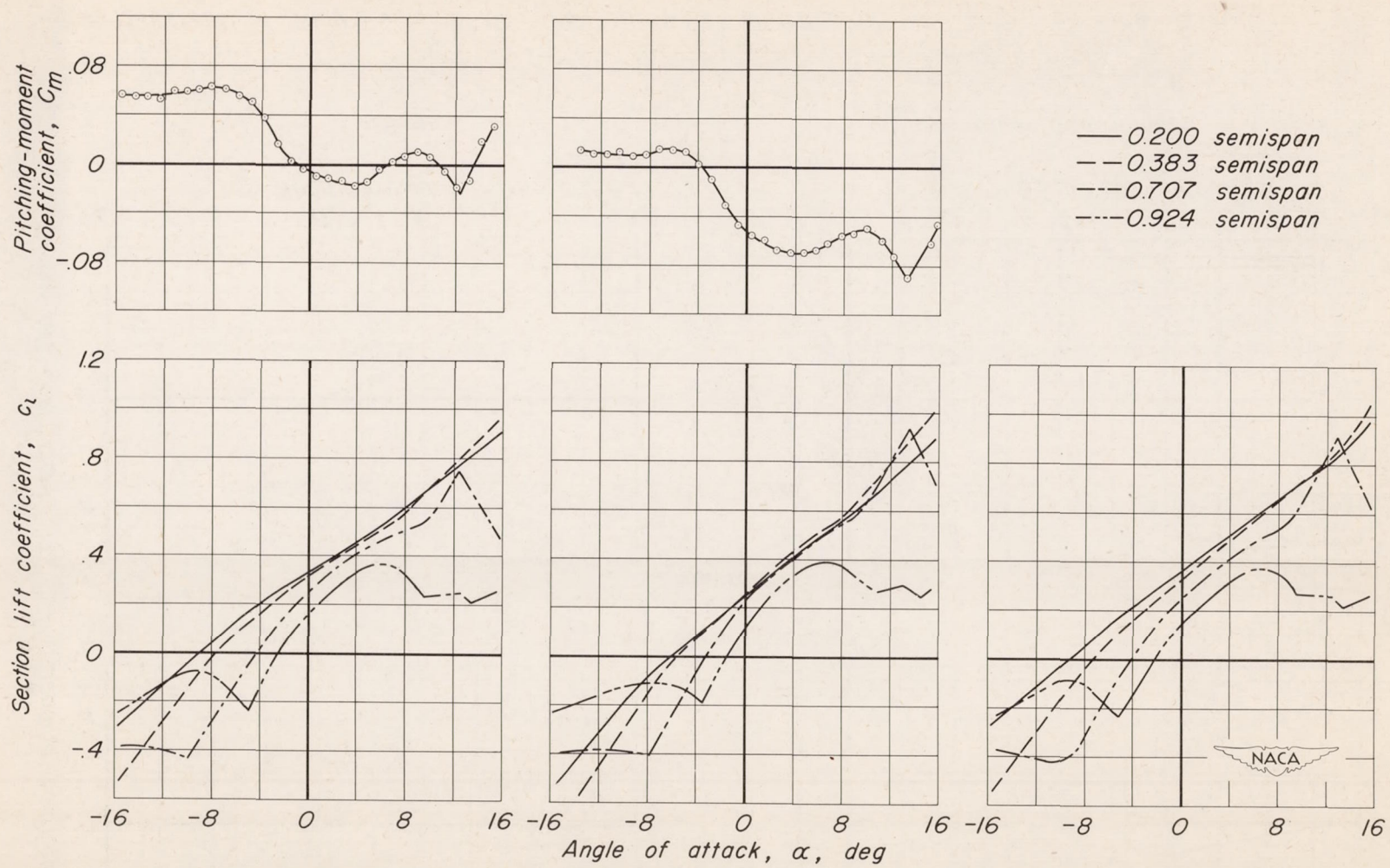

(a)Wing. (b)Wing with fuselage. (c)Wing (floor gap sealed).

Figure 12.-Variation of pitching-moment and section lift coefficients with angle of attack.

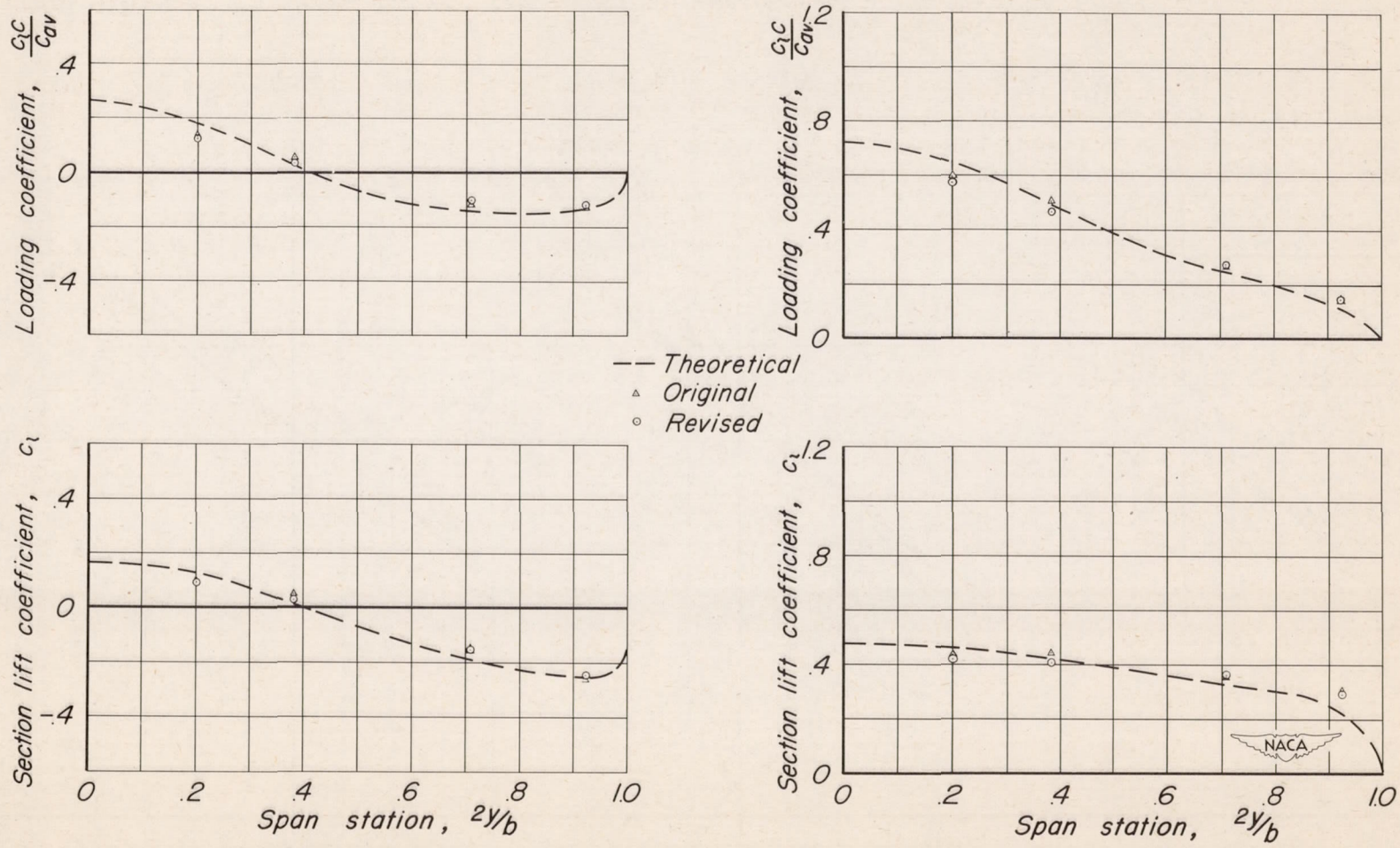

Figure 13.-Effect of wing revision on the spanwise distribution of load on the wing.